THE UNIVERSITY OF ALBERTA

A RETRACTABLE PROPULSION UNIT FOR A SELF-LAUNCHING SAILPLANE

by

© VINOD KUMAR SHARMA

A THESIS

SUBMITTED TO THE FACULTY OF GRADUATE STUDIES AND RESEARCH

IN PARTIAL FULFILMENT OF THE REQUIREMENTS FOR THE DEGREE

OF MASTER OF SCIENCE

DEPARTMENT OF MECHANICAL ENGINEERING

EDMONTON, ALBERTA

FALL, 1976

ABSTRACT

A retractable propulsion unit was designed and built for installation in a high performance sailplane. This unit will provide self-launching capability and at the same time maintain the soaring performance of the sailplane. In the design presented here, the motor remains fixed in the fuselage and only the propeller mounted on a pylon is extended for powered flight.

A 23 horsepower engine driving a 4 1/2 foot diameter propeller by means of a timing belt drive with 2:1 speed reduction would give take off and climb performance better than minimum specified by Organisation Scientifique et Technique Internationale du Vol a Viole air worthiness requirements.

Wind tunnel tests verified the performance characteristics calculated for this unit. The maximum thrust to power ratio was found to be 9.7 pounds per horsepower.

ACKNOWLEDGEMENTS

The author wishes to express his gratitude to Dr. D.J. Marsden for providing the opportunity to undertake this project and for his guidance and supervision of this thesis. Financial support for this project by the National Research Council is gratefully acknowledged.

Thanks are extended to the staff members of Mechanical Engineering shop, especially P. Bradbury and Tony Dyke.

Jim Kennedy and Dennett Netterville are remembered for their interest and suggestions at various stages of this project.

TABLE OF CONTENTS

LIST OF FIGURES

LIST OF SYMBOLS

a	induced velocity factor
A	frontal area of the pylon, $ft.^2$
b	circulation factor around a blade element
B	number of blades of propeller, in Chapter V; barometric pressure, inches of Hg, in Chapter VI
c	chord of blade element, ft.
C_d	drag coefficient of the glider
C_d^1	drag coefficient of the pylon
C_L	lift coefficient of the glider
D	drag of the glider, pounds
E	modulus of elasticity of steel, psi
F	load on the pylon, pounds
I	moment of inertia of cross-section about x-axis
K	correction factor for engine power
L	lift of the glider
$\dot{m}$	mass flow rate
M	mach number
N	rpm
p	interface pressure between clutch shoe and friction drum

P	power, h.p.
r	radius of a blade element from the hub center
R	inside radius of the friction drum contained in the smaller sprocket
t	ambient temperature, °F
T	thrust, pounds
v	climb rate, ft./sec.
V	forward velocity
V_R	resultant air velocity for a blade element
w	width of the friction surface
W	weight of the glider
α	angle of attack
Δ	deflection of free end of the pylon
γ	angle between the resultant aerodynamic force and the lift component on a blade element
ϕ	- angle of bank of an aeroplane in Chapter IV - angle of resultant air velocity with the plane of rotation of the propeller, in Chapter V
θ	- angle of climb, in Chapter IV - angle of zero lift line from the plane of rotation, in Chapter V
τ	Torque, in.-lb.
ω	angular velocity, radians per second

CHAPTER I

INTRODUCTION

Gliders were first used as a stage in the development of powered aircraft. For example the Wright brothers built and flew a glider before they added a motor. In that sense their first aircraft was a powered glider. Development of powered aircraft and sailplanes followed a divergent path after that.

Modern sailplanes are very efficient and have good handling characteristics that make them a delight to fly, but they have a major disadvantage that places limitations on their use. They have to be towed by an aeroplane or winch and are unable to return to the base if thermals should prove uncooperative. The use of an auxiliary motor for self-launching would greatly extend the utility of a sailplane.

A self-launching sailplane combines the convenience of operation of powered aircraft with the desirable features of the sailplane. This would greatly increase utilization and opportunity for cross-country flight compared to the "pure" sailplane. It would open up the sport of soaring to many who enjoy flying but cannot afford the investment of time necessary to fly the conventional sailplanes. A competition pilot could use it to gain experience

and practice cross-country tactics. Moreover, motorgliding would cut down the cost of this sport considerably.

Though motorgliders are being used in increasing numbers in recent years, their uses apart from the training role have not been developed very much. Some exceptions that may be noted are Nelson's Hummingbird, Motor Nimbus-2, SF-27M and ASK-14.

The Motor Nimbus-2, the SF-27M and the Hummingbird have retractable propulsion units which fold inside the fuselage behind the cockpit, while ASK-14 has a full feathering propeller mounted at the nose, as it is in conventional aircraft.

This thesis presents the design and development of an experimental unit which will power a two seater research vehicle, "Gemini". This unit employs a 27 horse power, two stroke engine and a 54 inch diameter propeller. The propeller retracts behind the cockpit. This unit was tested in the low speed wind tunnel, to investigate the reliability of the complete unit and to measure thrust developed and power consumed.

CHAPTER II

MEANS OF PROPULSION

2.1

The following means of propulsion have been used to propel the gliders:

i. Rocket

ii. Pulse Jet

iii. Turbojet

iv. Ducted Fan

v. Propeller

2.1.1 Rocket Engine

The first use of rockets to propel a glider was made by Fritz Opel, about 40 years ago. The early tests did establish the feasibility of this method of glider launching, but rockets are not economically competitive with other means of propulsion.

Solid propellent type rockets can be very small in size and light in weight for sufficient thrust to launch a glider. Their operating time is usually 10 to 15 seconds and their thrust is not controllable.

On the other hand, a typical liquid fuel rocket installation, gulping 18 gallons of monopropellent in five minutes, can give 100 pounds of static thrust, thus consum-

ing about 160 pounds of fuel and leaving about 35 pounds of powerplant hardware.

High fuel cost offsets the low initial cost of the hardware. Moreover, because of high fuel consumption the range is limited to very little more than a single launch.

2.1.2 Pulse Jet Engine

A pulse jet engine, operating on LP gas, can produce up to 80 pounds of static thrust. It has instant start capability and is controllable from 50 to 100 percent thrust. The World War II "buzz bomb" is a well known example of the use of a pulse jet engine.

The following disadvantages render it unsuitable for the purpose of propulsion of a glider. It has a high rate of fuel consumption and it is extremely noisy. The aft fuselage and tail surfaces must be kept clear of the hot jet wash. A pulse jet engine is bulky in size, so cannot be retracted in the fuselage.

2.1.3 Turbojet Engine

The turbojet engines too are not suitable for the gliders.

A major disadvantage of the turbojet engines is its relatively high fuel consumption rate, of the order of 1.5 pounds per pound thrust per hour. Range would be limited by the weight of fuel that could be carried. The

propulsive efficiency of a turbojet engine increases with flight speed. Since the flight speed of gliders is much below that at which the turbojet engines start showing good efficiency, the propulsive efficiency will also be low.

Small turbojet engines suitable for the gliders, are not readily available and the high initial cost is a further disadvantage.

Turbojet engines have been used on Caproni A-21J, Heinkel Grief, ASK-14 and Huelter H-30TS, but only on an experimental basis. Production aircraft are not being made available with turbojet engines, probably because of the disadvantages listed above.

2.1.4 Ducted Fan

A ducted fan provides higher static thrust than a propeller of the same diameter, but it cannot be retracted inside the fuselage, thus it would cause the power-off soaring performance to decline considerably.

A ducted fan called SG-85, weighing 123 pounds, has been developed for quick installation on gliders. It delivers over 90 pounds of static thrust. Flight tests of this unit on a Blanik have shown the power-off glide performance to be poor due to the drag of the non-retractable propulsion unit.

2.1.5 Propeller

A propeller provides an efficient means of propulsion

over the speed range of high performance sailplanes. It offers high static thrust, which is quite desirable for operation from grass fields. It offers the advantage of being able to be feathered or retracted for low drag gliding operation.

A relatively low cost piston engine can be used to drive the propeller. The power to weight ratio of such an engine is about 0.5 h.p. per pound, and its low fuel consumption rate would allow economical operation of a motor-glider.

2.2 Conclusion

Considering the above discussed means of propulsion on the basis of power-off glide performance, performance over a suitable range of forward velocity, fuel consumption rate, initial cost and availability, it was decided to develop a system employing a propeller and a piston engine. A suitable propeller and engine can be matched to give optimum performance over a fairly wide range of air speed, from best climbing speed to cruising speed.

CHAPTER III

PROPELLER-PISTON ENGINE CONFIGURATION

Configurations with piston engine-propeller propulsion units that have been used are; a nose mounted engine similar to that used on light aeroplanes, a fixed propulsion unit mounted on a pylon near the center of gravity, and a retractable propulsion unit retracting into a space in the aft fuselage behind the pilot. A fourth possibility is a propeller mounted at the tail, driven by an engine mounted near the aircraft center of gravity.

A completely retractable propulsion unit is needed in the case of a high performance sailplane to avoid loss of performance in unpowered flight. This configuration has been used on a number of motorgliders.

The propeller may be coupled to the engine either directly or through a speed reduction drive, and the entire motor and propeller unit is retractable. While keeping the motor and propeller in a single unit has advantage of simplicity, it has some serious disadvantages as well. It would require wide cut out in the fuselage, and the movement of heavy weight of the engine would displace the center of gravity back and forth. Forces needed to extend the motor may require a hydraulic actuator or complex mechanical system.

Since the whole weight is mounted at the end of the pylon, it would require heavy support structure. High engine speed would restrict the diameter of the propeller to a relatively small size, thus offering low efficiency of the propeller.

Another drawback of this configuration is that the time for conversion from unpowered to powered flight is fairly long, and the engine could be started only when the pylon is fully extended. This operation gives a little feeling of insecurity as the engine may fail to start and the drag of the extended propulsion unit will result in a sharply increased rate of sink.

The disadvantages noted above could be avoided if the engine is fixed in the fuselage and only the propeller, mounted on a suitable pylon, is extended for powered flight. The movable weight is reduced by about 70 percent, and the width of the cut out in the fuselage would be small.

This configuration requires a coupling between the engine and propeller drive. A centrifugal clutch would provide a suitable type of coupling and in addition it offers the advantage of allowing the engine to be started before the pylon is extended. If the engine fails to start, the pylon need not be extended, thereby avoiding any additional drag.

The design presented here was tailored specifically for the two place sailplane Gemini, which is described in Reference 3.

CHAPTER IV

POWER REQUIREMENT

Power required for the flight mode of an aeroplane as shown in Figure 1 is approximated by the following equation [1]:

$$P_{req.} = \frac{W\ V\ \text{Cos}\ \theta}{L/D\ \text{Cos}\ \phi}\left[1 + \frac{L}{D}\ \text{Cos}\ \phi\ \text{Tan}\ \theta\right]/550,\ \text{h.p.}$$

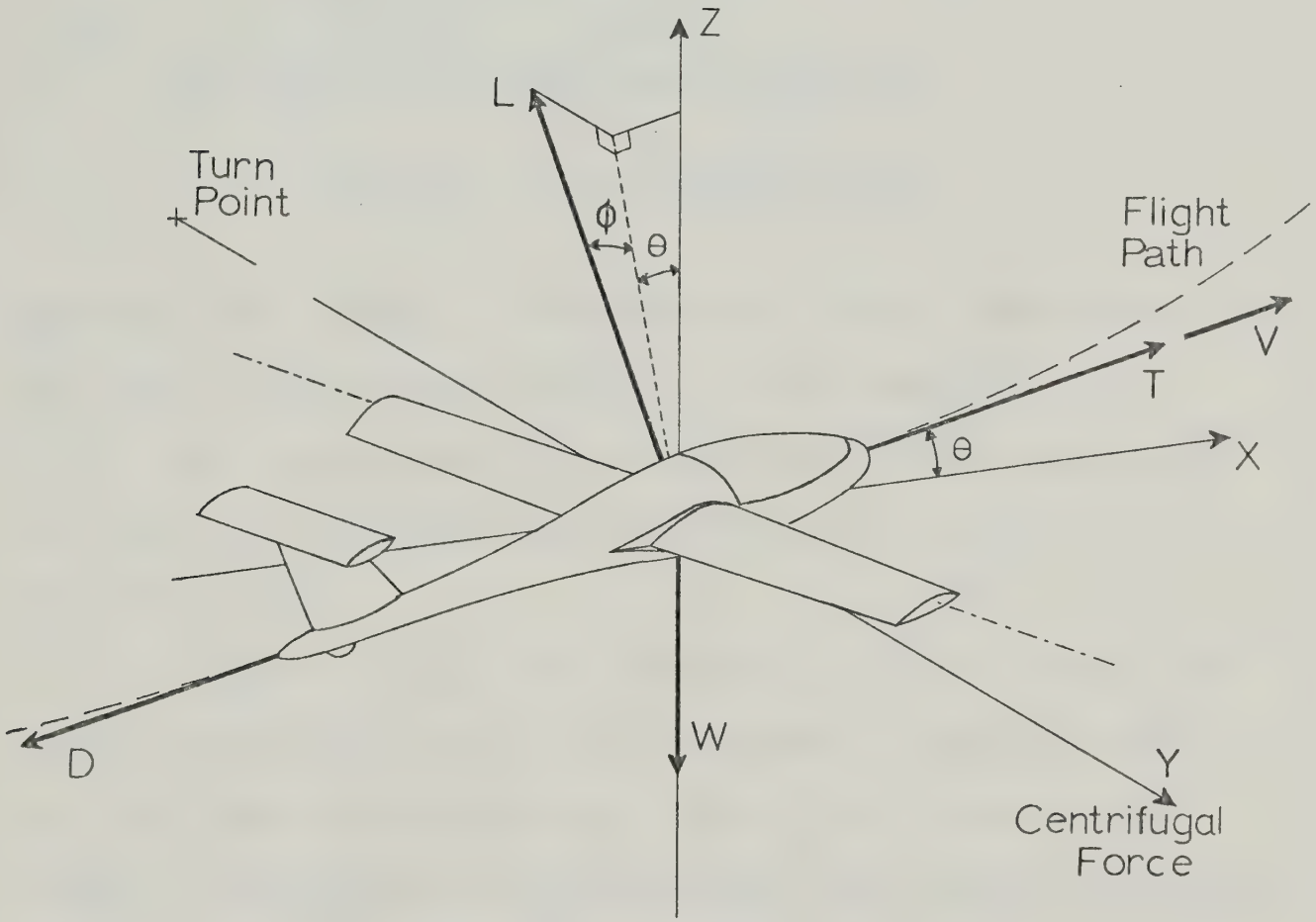

FIGURE 1, CLIMBING TURN

Considering straight flight without banking, and shallow angle of climb, less than 13°, the above equation was modified as:

$$P_{req.} = (DV + W\ V\ \text{Sin}\ \theta)/550,\ \text{h.p.}$$

where D = glider drag in level flight + pylon drag

$$= W \frac{C_D}{C_L} + \frac{1}{2} \rho\ C_D^1\ V^2\ A$$

C_D^1 = 1.2, pylon drag coefficient [2]

A = 1.26 ft.^{2}, pylon frontal area.

Writing V Sin θ as v, climb rate in ft/sec., the expression for power required was written as (DV + Wv)/550, h.p.

For calculation of drag of the Gemini, the values of C_D/C_L were obtained from its Glide Polar Data given in Appendix I [3].

Figure 2 shows the variation of total drag of the sailplane and the pylon, as a function of forward velocity, at 2,000 feet above sea level and 70°F air temperature. Figure 3 shows the thrust horsepower required for different climb rates, as a function of forward velocity.

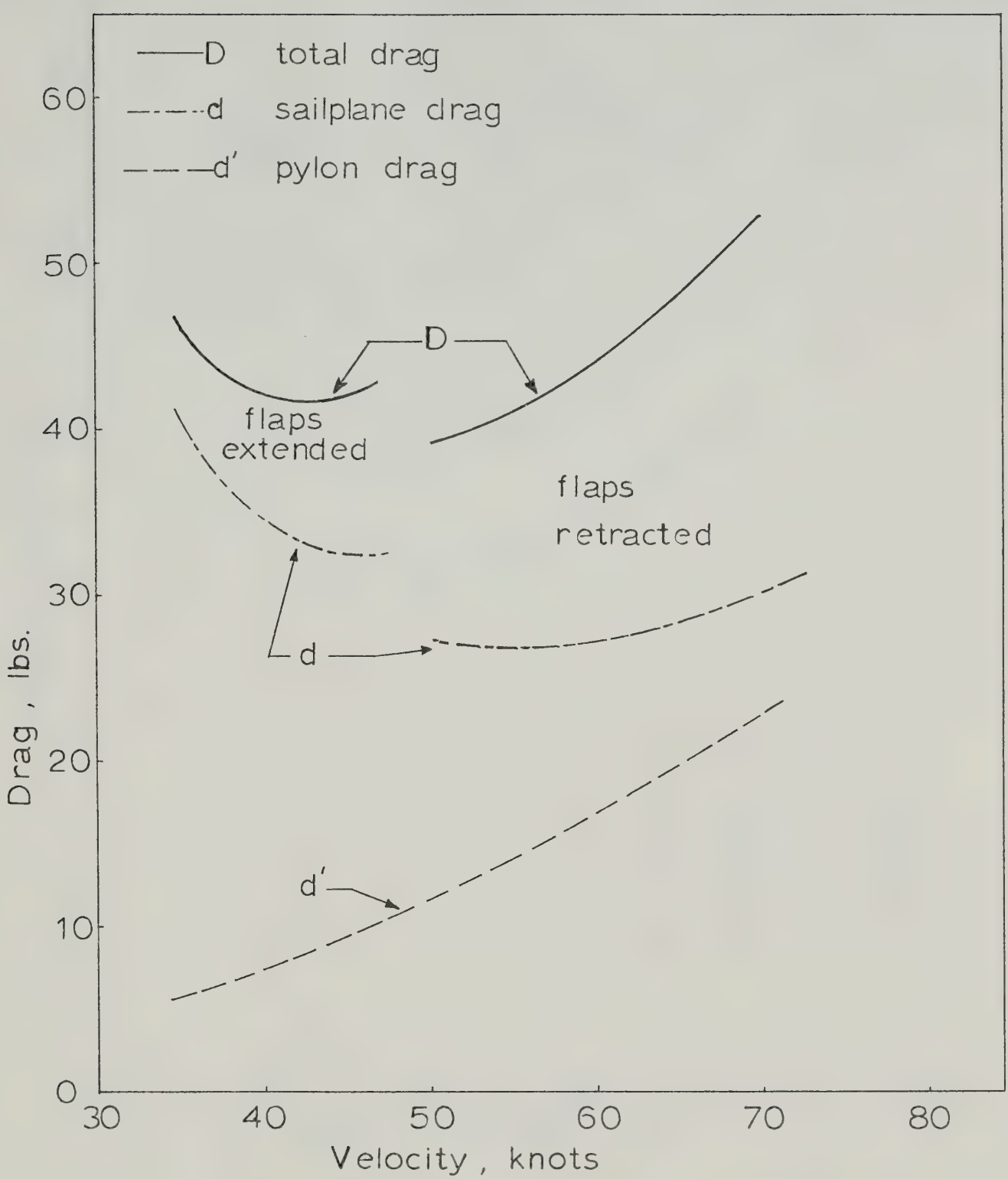

FIGURE 2, DRAG AS A FUNCTION OF FORWARD VELOCITY

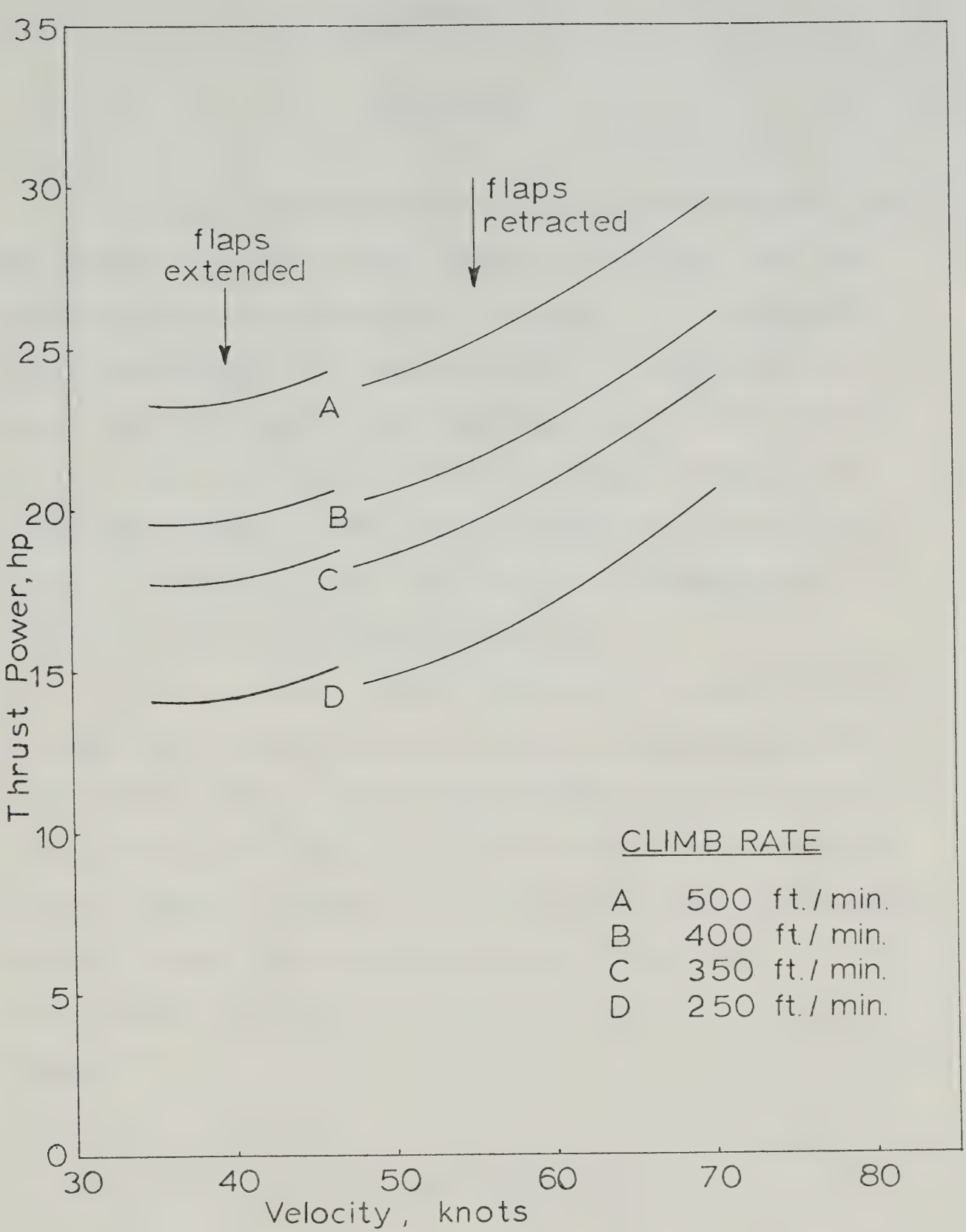

FIGURE 3 , POWER REQUIRED AS A FUNCTION OF FORWARD VELOCITY

CHAPTER V

PROPELLER

Froude's momentum theory of propulsion shows that the highest propulsive efficiency is achieved with the largest practicable propeller diameter. In the present case, the diameter of the propeller is limited by the space available inside the fuselage and by the condition that the tip velocity be limited to approximately 0.75 times the speed of sound. A 2:1 speed reduction allows a propeller speed of 3,000 rpm giving a tip Mach number of 0.62 for a 54 inch diameter propeller.

Blade element theory combined with momentum theory [4] was used to calculate the propeller characteristics shown in Figure 5. This theory permits a direct calculation of the performance of a given propeller, or can be used to design a propeller to achieve a given performance. Figure 4 shows the velocities, angles and forces on a blade element of length δr located at radius r. From Figure 4

$$\phi = \text{Tan}^{-1} \frac{V(1 + a)}{\omega r(1 - b)}$$

$$V_R = \frac{V(1 + a)}{\text{Sin } \phi} = \frac{\omega r(1 - b)}{\text{Cos } \phi}$$

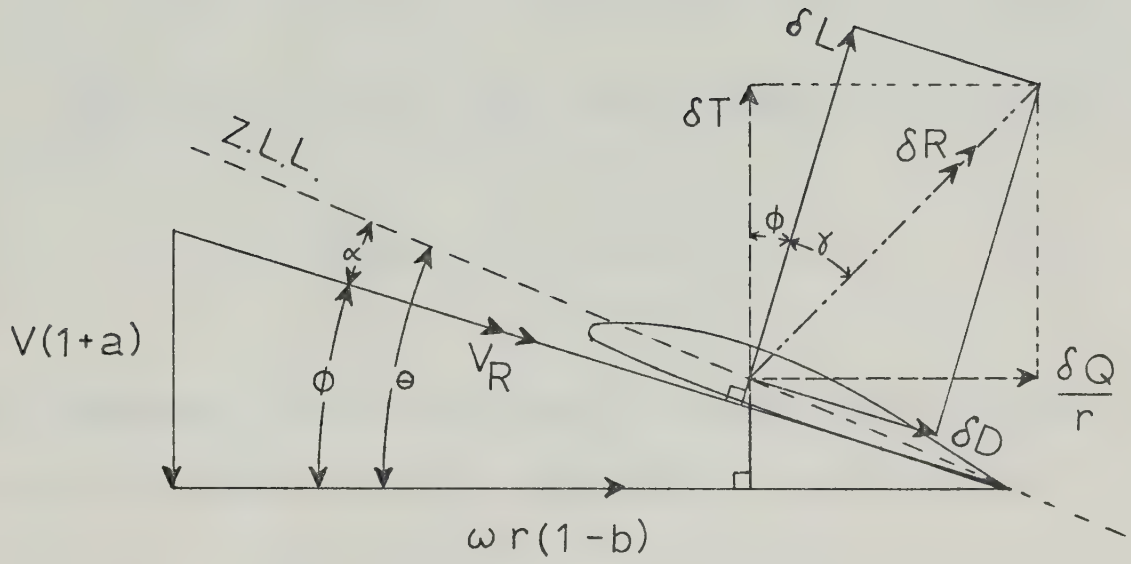

FIGURE 4. BLADE ELEMENT

$$\text{Tan } \gamma = \frac{\delta D}{\delta L} = \frac{C_D}{C_L} \qquad (5.1)$$

Lift of the element, $\delta L = \frac{1}{2} B\ c\ \delta r\ \rho\ V_R^2\ C_L$, and drag of the element, $\delta D = \frac{1}{2} B\ c\ \delta r\ \rho\ V_R^2\ C_D$. The thrust component of the element is:

$$\delta T = \delta L \text{ Cos } \phi - \delta D \text{ Sin } \phi$$

and the torque force component is:

$$\frac{\delta Q}{V} = \delta L \text{ Sin } \phi + \delta D \text{ Cos } \phi$$

Simplifying the thrust component, introducing solidity, $\sigma = \frac{B\ c}{2\pi r}$, and substituting for C_D from equation 5.1:

$$\frac{dT}{dr} = \pi\ r\ \sigma\ \rho\ V_R^2\ C_L \text{ Sec } \gamma(\text{Cos } \phi \text{ Cos } \gamma - \text{Sin } \phi \text{ Sin } \gamma)$$

$$= \pi\ r\ \phi\ \rho\ V_R^2\ C_L \text{ Sec } \gamma \text{ Cos}(\phi + \gamma)$$

For moderate angles of attack of the blade sections, Tan γ is small, about 0.02 for L/D = 50:1, and therefore Sec γ = 1. Thrust Grading is given by:

$$\frac{dT}{dr} = \pi\ r\ \phi\ \rho\ V_R^2\ C_L \text{ Cos}(\phi + \gamma) \qquad (5.2)$$

and similarly Torque Grading is:

$$\frac{dQ}{dr} = \pi\ r^2\ \sigma\ \rho\ V_R^2\ C_L \text{ Sin}(\phi + \gamma) \qquad (5.3)$$

considering the axial momentum of the flow through the annulus. Thrust δT is equal to the product of rate mass flow ($\dot{m}$) through the annulus with the change in axial velocity (δV)

$$\delta T = \dot{m} \times \delta V$$

$$= 2 \pi r \delta r \rho V(1 + a)2 a V$$

$$\therefore \frac{dT}{dr} = 4 \pi \rho r V^2 a(1 + a) \qquad (5.4)$$

Comparing the equations 5.2 and 5.4:

$$\frac{a}{1+a} = \frac{1}{4} \sigma C_L \text{Cos}(\phi + \gamma)\text{Cosec}^2 \phi \qquad (5.5)$$

Next considering angular momentum: $\Delta\omega$ is the change in angular velocity of air passing through the annulus and is equal to 2 b ω

$$\delta Q = \dot{m} \Delta \omega r^2$$

$$= (2 \pi r \delta r)[\rho V(1+a)](2 b \omega)r^2$$

$$\frac{dQ}{dr} = 4 \pi r^3 \rho V b(1 + a)\omega \qquad (5.6)$$

Comparing equation 5.3 to 5.6:

$$\frac{b}{1-b} = \frac{1}{2} \sigma C_L \text{Sin}(\sigma + \gamma)\text{Cosec } 2\phi \qquad (5.7)$$

The lift curve slope of the propeller blade is calculated to be 0.1 per degree [4,5]. The compressibility effect changes this by a factor $1/\sqrt{1-M^2}$, given by the Prandtle-Glauert correction, provided $M < 0.75$. In the present case the maximum Mach number is 0.62, therefore the above correction is applicable.

The propeller blade was divided into nine elements, each two inches long, from a radius of nine inches to the tip.

The following procedure was used to calculate the thrust developed and the power required by each element.

i. Assume a = 0.1 and b = 0.01.

ii. Values of ϕ, V_R, C_L and α are calculated, applying the compressibility correction.

iii. a and b are calculated with the help of equations 5.5 and 5.7. These new values of a and b are compared with the assumed ones in step (i). If the difference exceeds $\pm 10^{-5}$, the process is repeated with new starting values taken to be the mean between previous starting values and calculated values of a and b.

iv. Using equations 5.2 and 5.3, thrust grading and torque grading are calculated.

v. The above steps are followed for each of the nine elements. Graphs are plotted of thrust grading and torque grading versus radius.

The area under the first curve gives the total thrust of the blade, and that under the second curve gives the torque required.

A computer program was developed to do the iterative computations for values of a and b. This theory holds good in the range $0 < a \leq 1$, i.e., the inflow velocity is positive and smaller than the forward velocity. The thrust curve between zero forward velocity and the velocity at which a approaches 1, is extrapolated so that thrust variation with velocity is approximated by the following equation [3]:

$$T = T_0 - C V^2 \qquad (5.8)$$

where T_0 is the thrust at zero forward velocity, and T is the thrust at V feet per second. C is a constant.

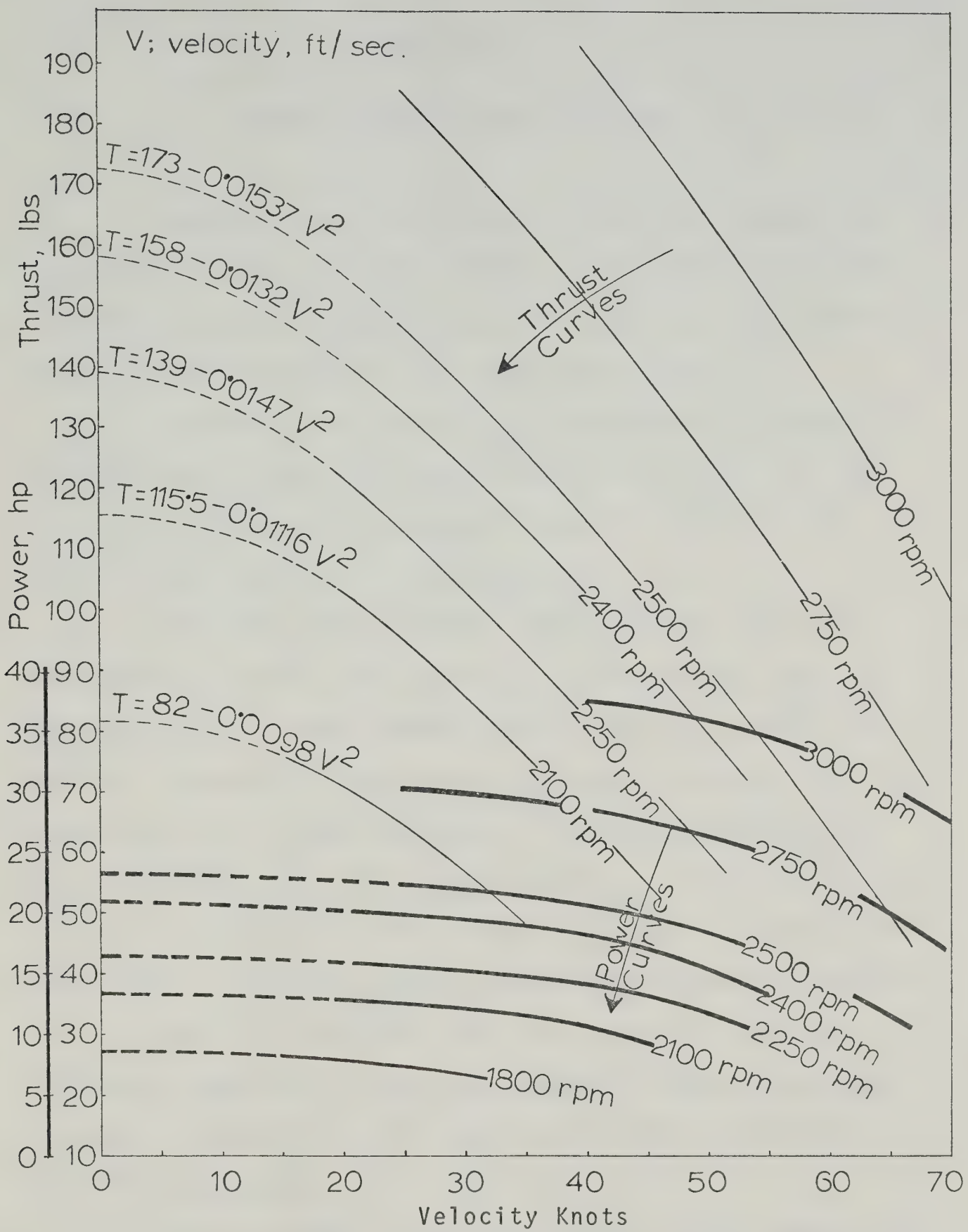

FIGURE 5 , PROPELLER CHARACTERISTICS

CHAPTER VI

ENGINE SELECTION AND TESTING

The weight of the engine usually constitutes 55 to 60 percent of the total weight of the propulsion unit. Therefore suitable selection of the engine is very important to keep the weight of the whole unit down.

According to Figure 3, 25 horsepower is needed for a climb rate of 500 feet per minute at 55 knots. If the propeller efficiency is assumed to be 70 percent, the engine power required is 36 horsepower.

Two cycle, two cylinder small engines (25 to 50 horsepower) produce peak power at 5,000 to 6,000 rpm, thus requiring a speed reduction of about 2:1 at the propeller. Snowmobile engines and motorcycle engines provide a good variety of such engines. The Wankel engines have some advantages over the piston engines in terms of vibrations and compactness, but piston engines are readily available while a suitable wankel engine could not be obtained.

Motorcycle engines were not considered because forced air cooling of the type commonly found in snowmobile engines is needed for this application where the engine is internally mounted.

A two cylinder, two cycle KOHLER 4402AX engine was selected. Specifications for this engine are given in

Appendix III.

Proper tuning of the exhaust system in two cycle engines is quite important. When the exhaust port opens at 80° bBDC,* a pressure pulse travels along the exhaust pipe. At the end of the exhaust pipe, it is reflected back as a rarefaction wave. For good scavenging and pulse charging, this rarefaction wave should reach the port when the piston is in the vicinity of BDC. Accordingly, an optimum length of pipe was found to be 22 inches, for the engine to operate at 6,000 rmp. This length would increase for lower speed operations.

Figure 6 shows the comparison of the measured power with the manufacturer's rating of the engine. The measured power output is considerably less than the advertised one.

The following formulae was taken from SAE TEST CODE J607, to find the correction factor for correcting the rated power for existing conditions:

$$K = \frac{B - E}{29.92} \times \frac{520}{460 + t}$$

B = observed barometric pressure in inches of Hg

E = water vapour pressure in inches of Hg

t = carburetor air temperature in F.

The correction factor K was found to be 0.886 for 70°F and

---

* bBDC - before Botton Dead Center.

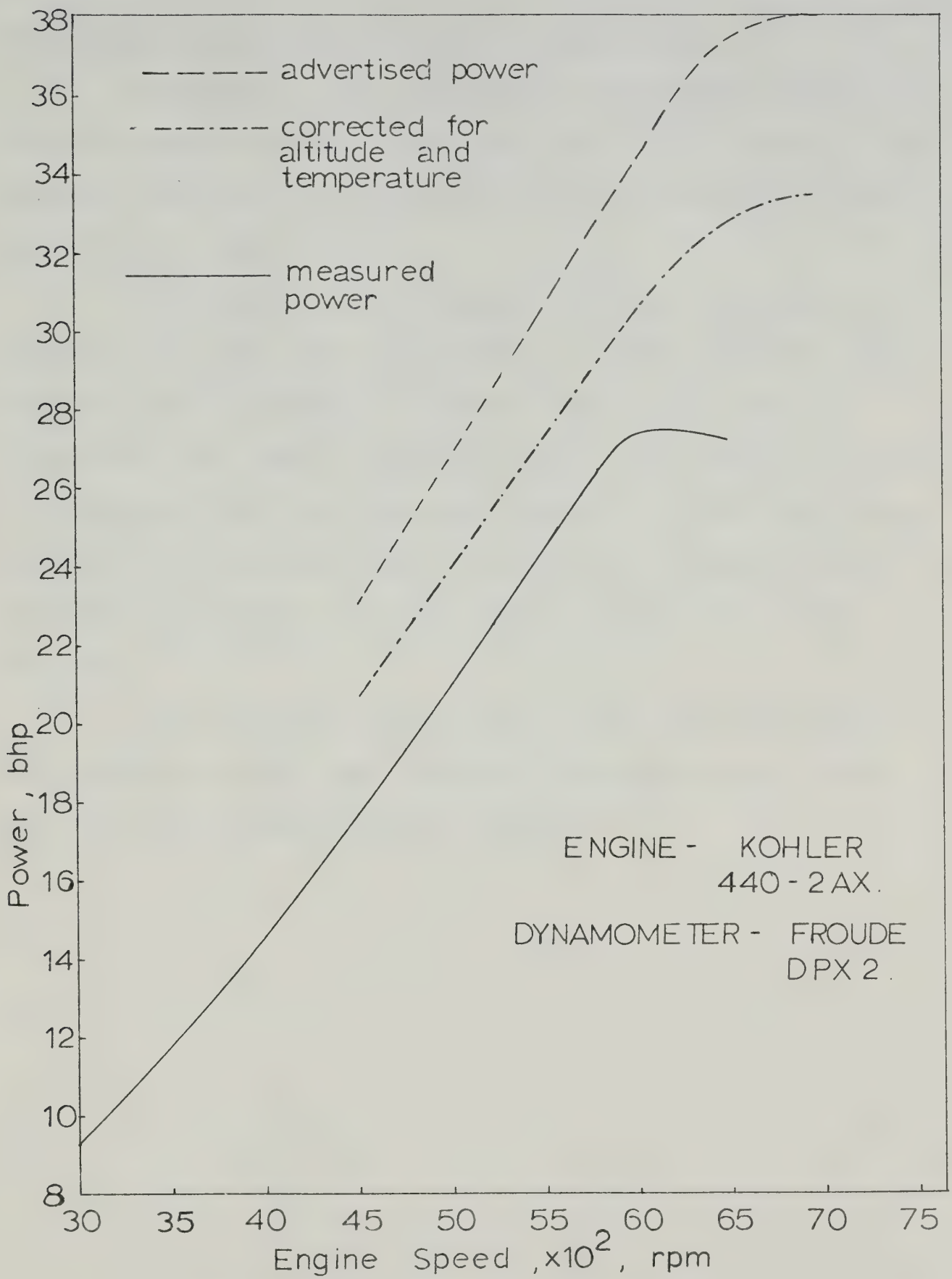

FIGURE 6, ENGINE POWER

the barometric pressure of 27.5 inches of Hg.

According to the test code, the engine should produce 85 percent of the rated power till it is run-in. The engine, after run-in should produce not less than 95 percent of the rated power.

The maximum power measured at 6,000 rpm, was 12 percent less than the rated power. Though the engine was run for about 15 hours, it had not been fully run-in. Therefore, the power output was within the limits prescribed in the test code, but the power peaked at 6,000 rpm instead of 7,000 rmp as advertised. Any specific reason of the discrepancy between the peak powers, could not be established.

From Figures 5 and 6, we see that the motor will not produce enough power to turn the propeller at 3,000 rpm at flight speeds below 70 knots.

CHAPTER VII

DESIGN OF THE RETRACTION MECHANISM AND THE COMPONENTS

7.1 General

The simplest retractable mechanism can be a hinged pylon carrying the propeller at the free end. The pylon may be raised or lowered with the help of a hydraulic system. There is a major disadvantage in this type of mechanism. It requires a long cut out in the fuselage, at least equal to the diameter of the propeller. This opening in the fuselage would demand reinforcement of the structure. Moreover, in Gemini there is a main bulkhead which joins the tail cone to the main body (Figure 7). It is undesirable to cut this bulkhead in order to keep its strength without adding any weight in reinforcement.

A system shown schematically in Figure 7 was devised to keep the opening in the top of the fuselage short. The lower end of the pylon is driven along a guide track by a 12 VDC motor driving a pinion through the reduction gear ratio of 30:1. The pinion runs on a rack laid on the guide track. This mechanism allows the cut out to be only a little longer than half of the propeller diameter.

A limit switch stops the pylon in the final vertical position and a spring loaded latch (Figure 8) locks

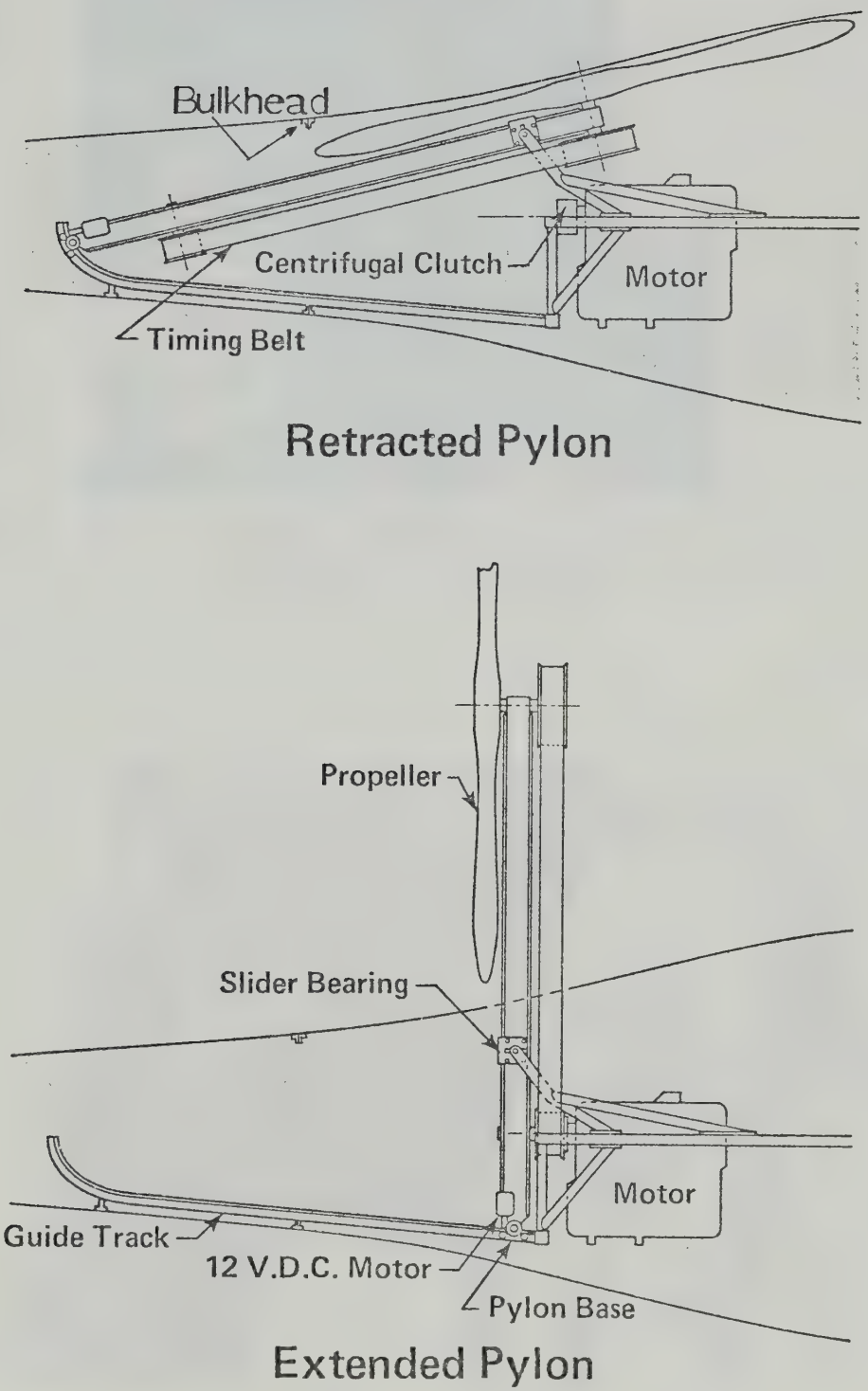

Figure 7 . Schematic Diagram of the Propulsion Unit

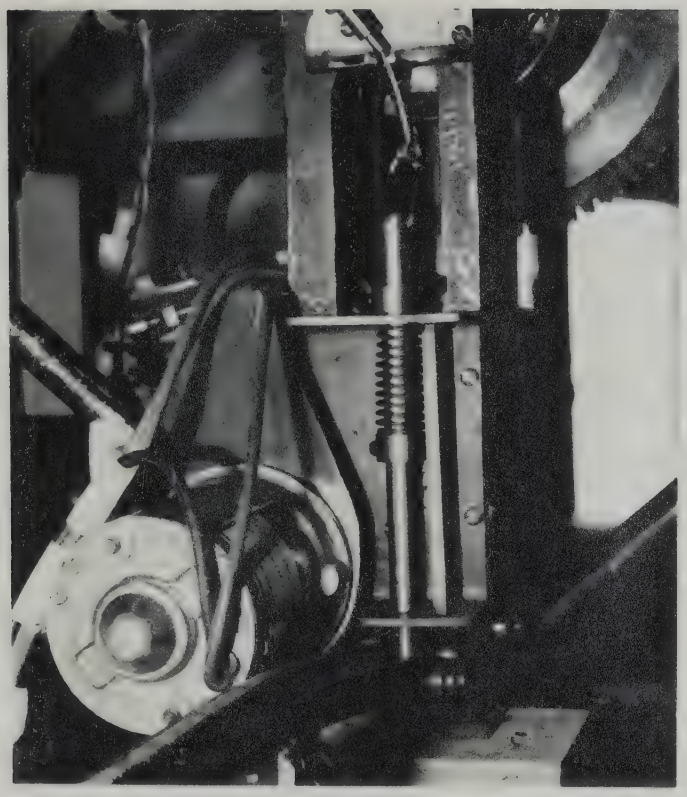

FIGURE 8 , SPRING LOADED LATCH , PYLON IS LOCKED IN UPRIGHT POSITION

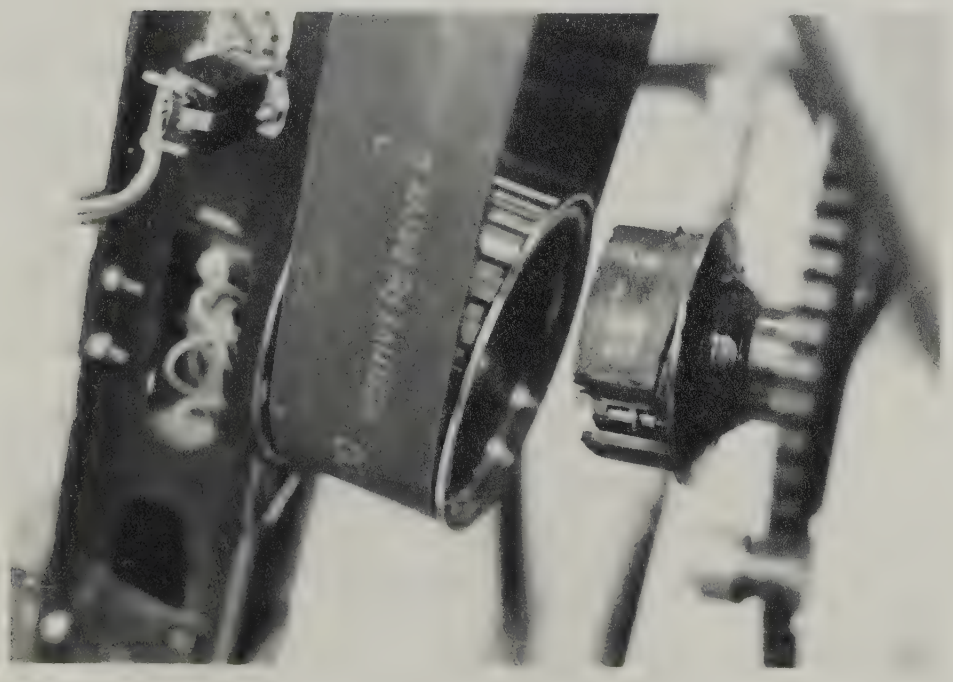

FIGURE 9 , PHOTOGRAPH SHOWING LOWER SPROCKET COMING IN TO COVER CENTRIFUGAL CLUTCH

the pylon in this position. In order to have no interference between the drum and the rotating shoes of the clutch, the initial radial clearance is 1/4". The profile of the guide track was modified so that during insertion, the drum forms an arc about the pivot point of the upper support of the pylon. Figure 9 shows the lower sprocket (containing the clutch drum) coming in to cover the centrifugal clutch.

Figure 10 shows an exploded view of the pylon.

7.2 Pylon

The plyon which carries a maximum load of about 250 pounds of thrust concentrated at the free end, was designed to deflect no more than 5/16" under 250 pounds load.

Using the Dummy Load method [6], the deflection of the free end of a beam of uniform cross-section is given by:

$$\Delta = \frac{F}{3\ E\ I} (\ell^3 - \ell_1^3 + \ell_1 \ell_2^3 - 3\ L\ \ell_1 \ell_2)$$

where ℓ = Total length of the pylon

ℓ_1 = Distance between the two supports

ℓ_2 = Distance from the upper support to the free end.

The maximum moment of inertia of the cross-section

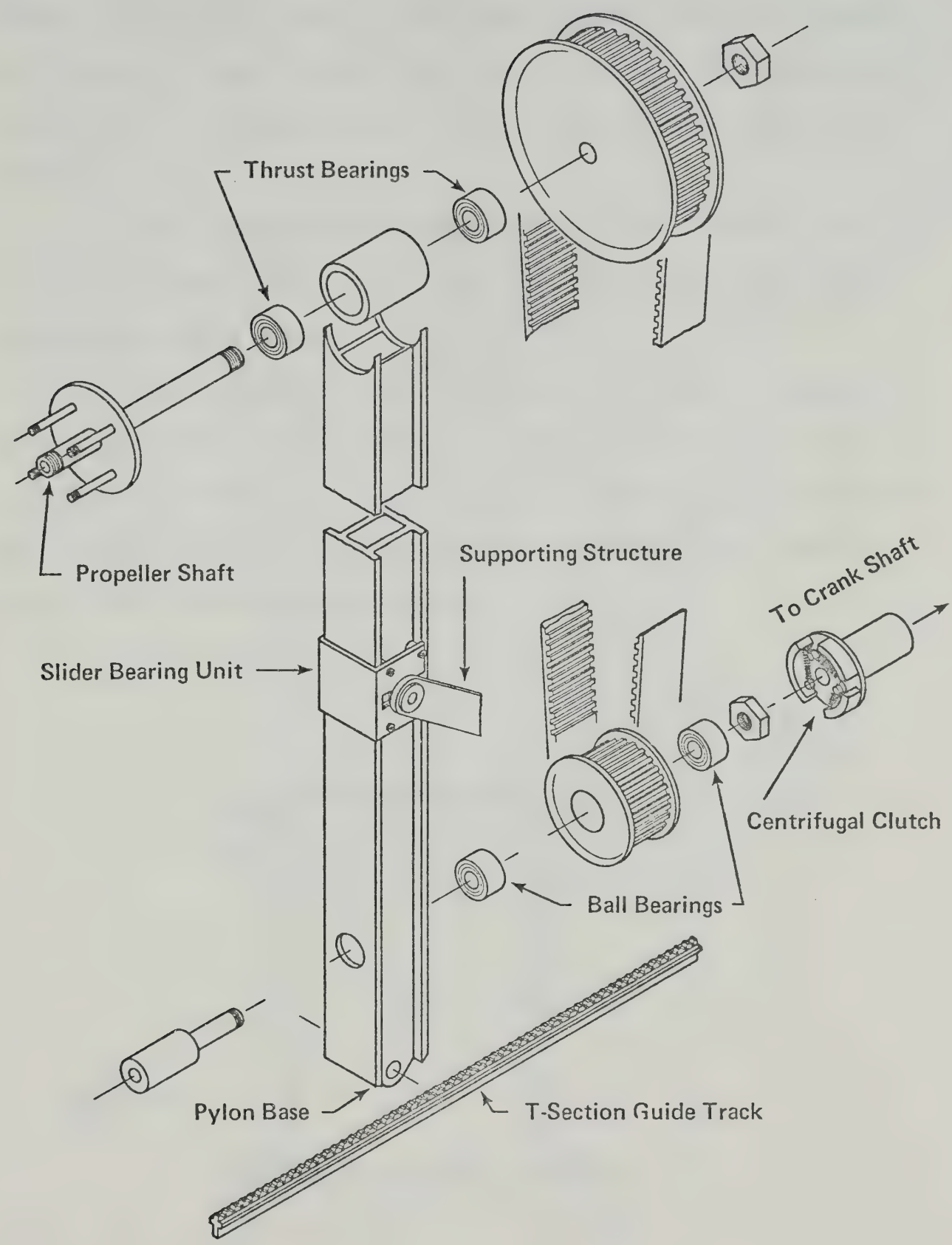

Figure 10 , Exploded View of Pylon

needed to meet the above requirement for deflection was found to be 0.57 inch.[4] A uniform cross-section as shown in Figure 10, was chosen for simplicity and high torsional stiffness. Its moment of inertia about X-axis was 1.113 inch.[4]

The static load testing indicated a deflection of 0.16 inch under 250 pounds load, in agreement with the equation stated above.

The weight of the pylon was 14 pounds. Lightening holes and slots were milled out as shown in Figure 12, to reduce its weight to 10.25 pounds. The free end deflection was found to be 0.29 inch under 250 pounds load, which satisfied the design criterion.

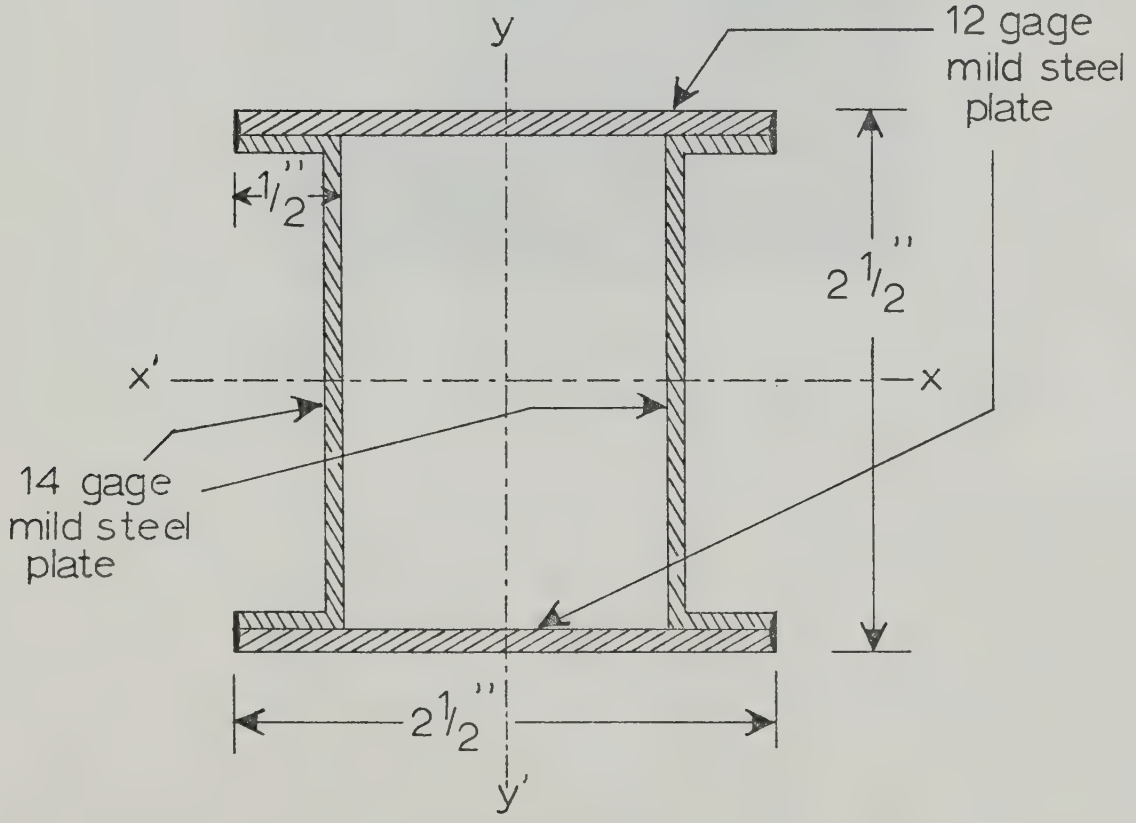

FIGURE 11. PYLON CROSS-SECTION

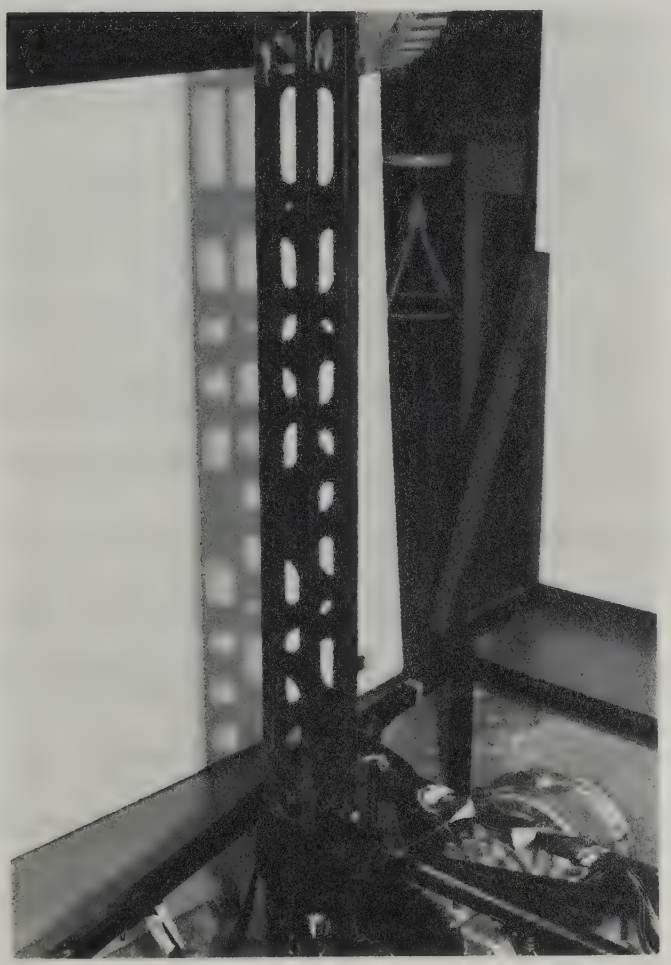

FIGURE 12 , PHOTOGRAPH SHOWING LIGHTENING HOLES AND SLOTS IN THE PYLON

Figure 13 shows the details of the slider bearing which provides the upper support for the pylon. The maximum forward load at this support is 750 pounds, about three times the maximum thrust. The cam followers R_1, R_2, R_3 and R_4 take up the forward load. Each one of them is capable of carrying 324 pounds of static load.

The cam followers R_4, R_6, R_7 and R_8 take up the drag load and R_9, R_{10}, R_{11} and R_{12} take up the transverse load of the pylon.

7.3 Centrifugal Clutch

Basic considerations:

i. The friction material is asbestos brake lining, giving a coefficient of friction of 0.32 when acting against the cast steel drum. The asbestos is chemically bonded to the mild steel shoes. The maximum allowable temperature is 475°F.

ii. The interface pressure at any point is proportional to the vertical distance [7] from the hinge pin (Figure 14). The maximum pressure [p_{max}] occurs at 90° from the horizontal line.

iii. The basic dimensions of the shoe were limited by the space available. The initial radial clearance between the shoes and the drum is 1/4" to prevent interference as the drum is

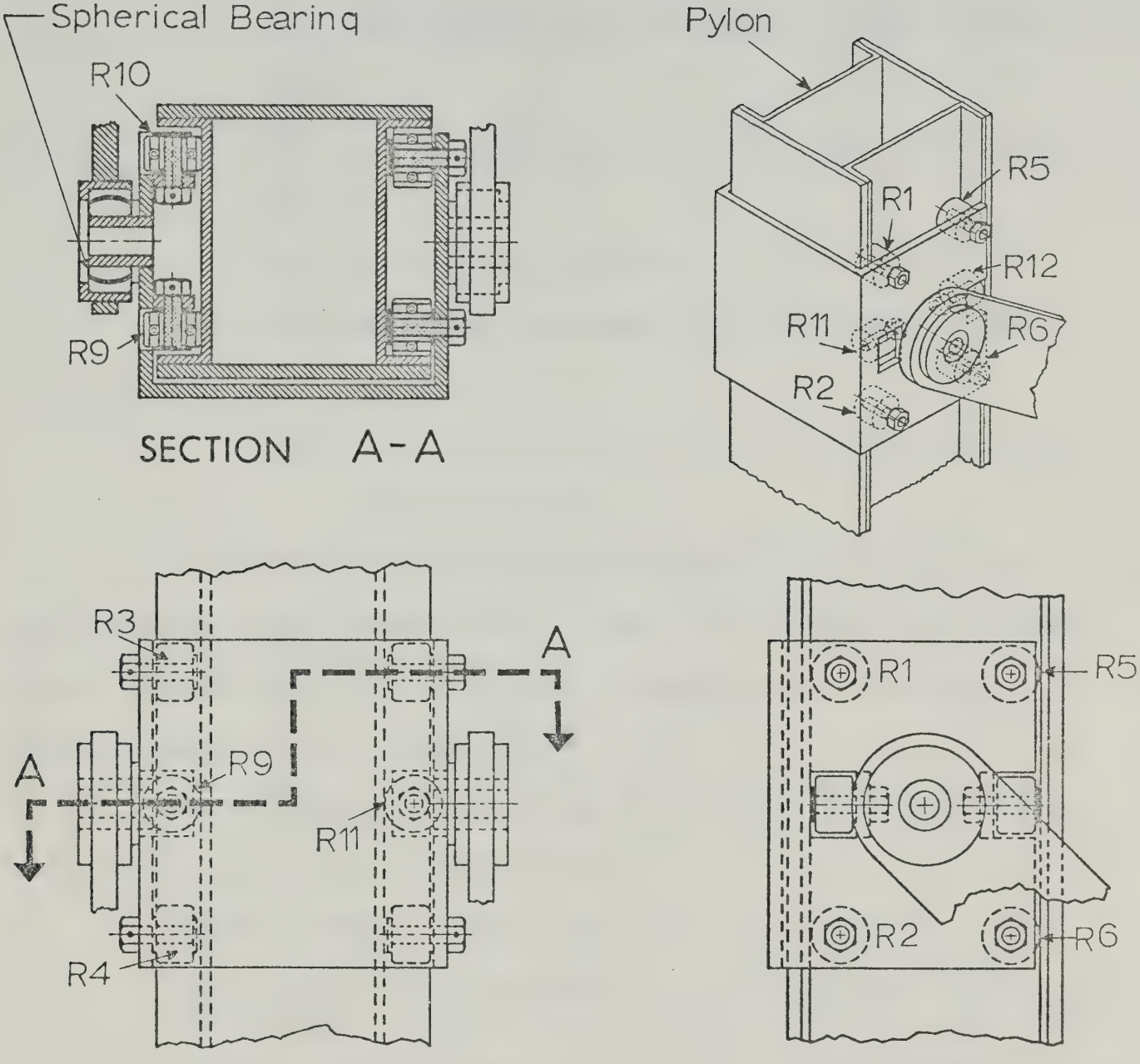

Figure 13 , Slider Bearing

moved over the clutch.

iv. The smooth idling speed of the engine is 1,400 rpm. The spring force should prevent the shoe from flying outwards, below 1,400 rpm.

v. The static analysis [7] would give the following data:

(a) Interface pressure.

(b) Maximum horsepower transmitted without slip.

(c) The speed at which the shoes just engage with the drum.

Iterative calculations were done to arrive at the appropriate basic dimensions of the shoe so that the horsepower transmitted by the clutch is matched to the power requirements of the propeller.

The following dimensions were determined in accordance with the above considerations:

Inside radius of the drum, R = 1.58 inches.

Location of the hinge pin, r = 0.9 inches from the center.

Width of the friction surface, w = 0.75 inches.

Angles of the friction material, subtended at the center were (Figure 14):

$$\beta_1 = 39^\circ \quad \text{and} \quad \beta_2 = 106^\circ$$

Total number of shoes = 3.

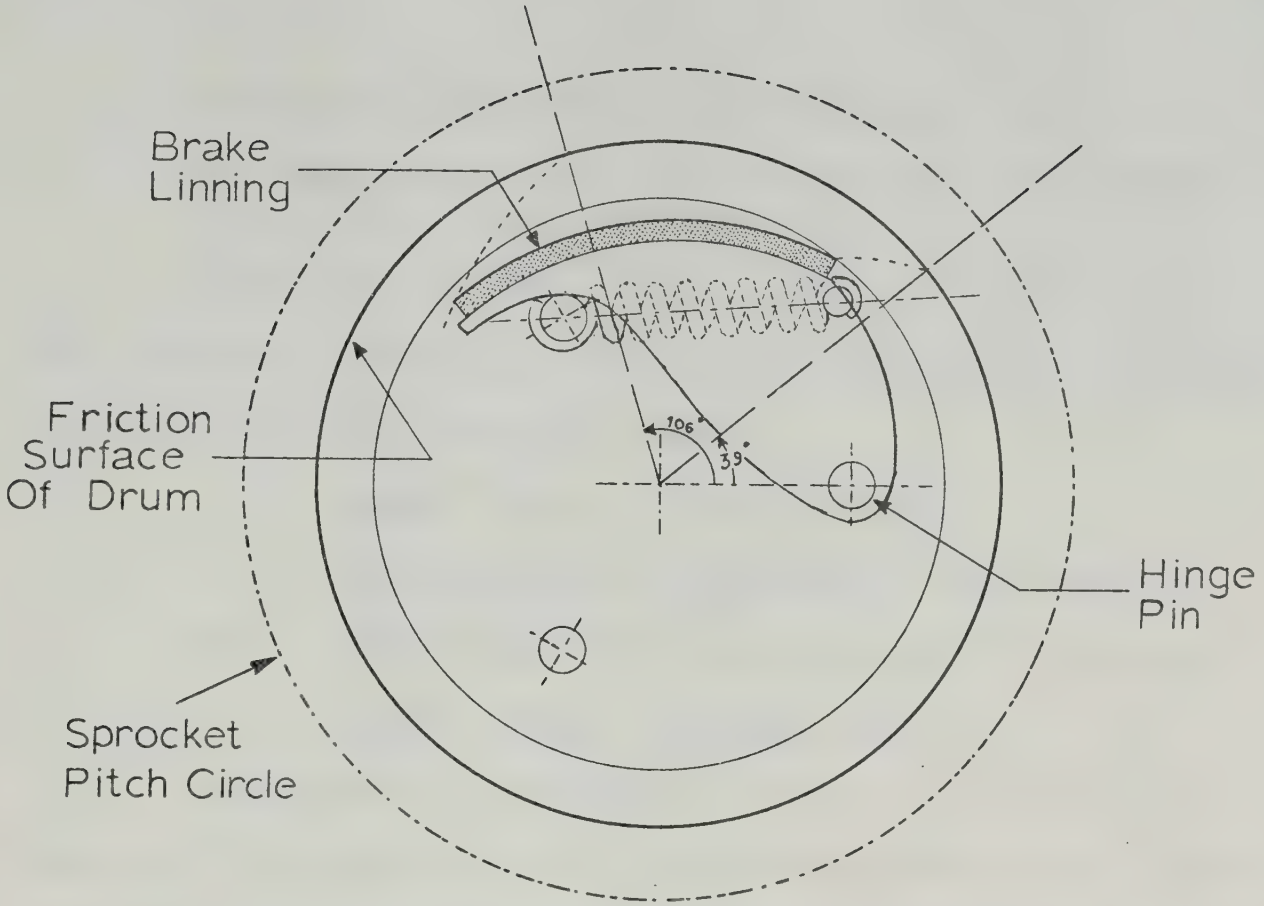

FIGURE 14·1, CENTRIFUGAL CLUTCH WITH SHOE IN CLOSED POSITION

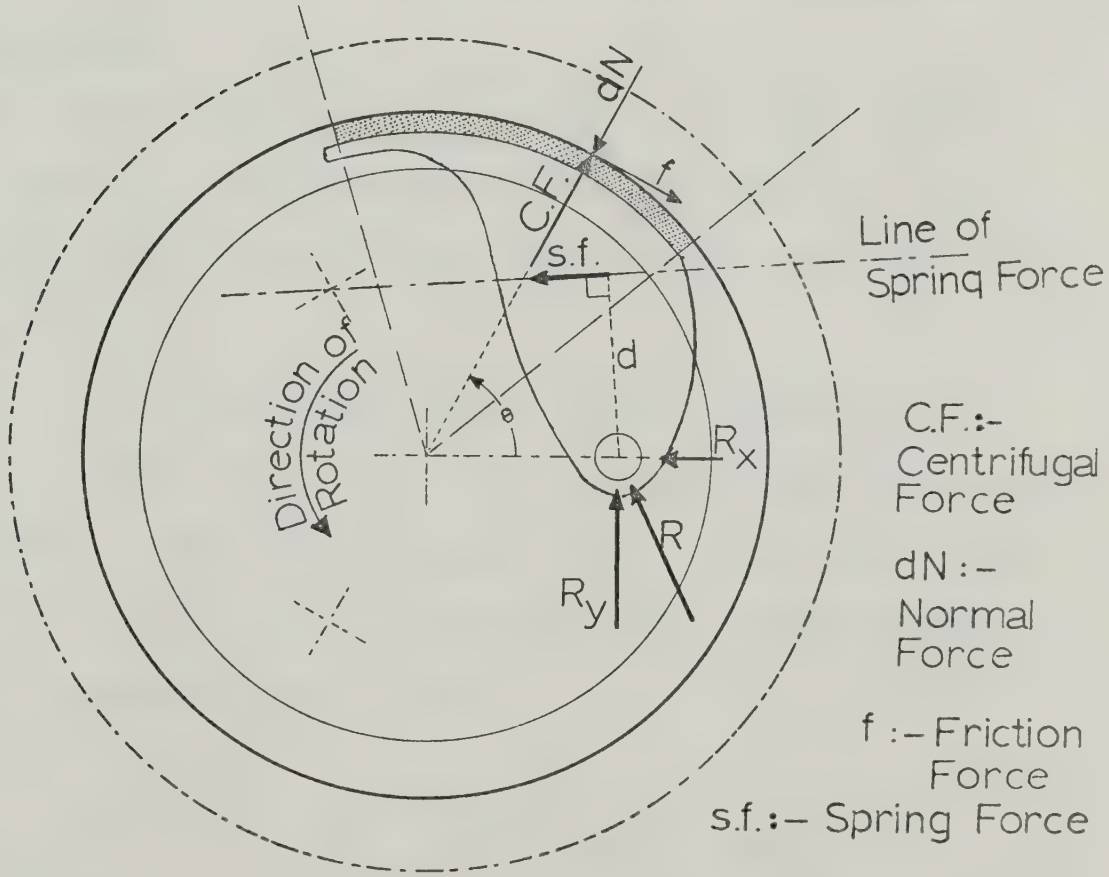

FIGURE 14, SHOE IN ENGAGED POSITION

Weight of each shoe = 0.190 pounds.

Maximum displacement of the spring = 0.3 inches along the line AB in Figure 14.

Moment arm of the spring force, d = 0.85 inches.

The following forces are involved when the shoe is engaged with the drum and transmits torque.

i. Normal force at the interface.

ii. Friction force tangential to the surface.

iii. Centrifugal force acting radially outward.

iv. Spring force along the line AB.

Considering an element of area w x R x $d\theta$ at an angle θ, the moments of the above mentioned forces, about the hinge pin were obtained. Their simple integration from $\theta = 39°$ to $\theta = 106°$ yielded the moments of these forces on the whole shoe.

The spring force needed to keep the shoes folded at idling speed was estimated by balancing moments about the hinge pin due to centrifugal force with those due to the spring force.

The springs selected had a spring constant of 20 pounds/inch. Allowing for initial spring tension with the shoes retracted, the following equation for maximum interface pressure was derived by balancing the moments when the shoe is in the engaged position:

$$p_{max} = 10.112 \times 10^{-6} \times N^2 - 25.39, \text{ psi}$$

where p_{max} is the maximum interface pressure and N is rpm of the clutch.

Maximum torque transmitted per shoe was obtained by integrating the torque due to friction over the length of the shoe from $\theta = 39°$ to $\theta = 106°$. The resulting torque was

$$\tau = 0.59155 \times p_{max}, \text{ lb-in.}$$

Therefore the maximum power transmitted per shoe is given by:

$$P = 0.9386 \times 10^{-5} \times N \times p_{max}, \text{ h.p.}$$

Table 1 was prepared with the help of the above equations. Figure 15 shows the comparison of the power transmission capability of the clutch with the engine power available and with the power required by the propeller.

The speed at which the shoes just engage with the drum was calculated to be 1,585 rpm while experimentally it was found to be 1,550 rpm.

The maximum hinge pin reactions are computed by summing up the components of all the forces, in X and Y directions. The resultant reaction on the hinge pin at 6,000 rpm was calculated to be 266 pounds. This reaction causes a shear stress of 3,500 psi in a hinge pin of 5/16" diameter.

TABLE 1

CLUTCH PERFORMANCE

Clutch Speed (rpm)	Maximum Interface Pressure, p_{max} (psi)	Maximum Torque Transmitted by Each Shoe (lb-in)	Maximum Horsepower Transmitted	
			Per Shoe	Total
2,000	15.06	8.90	0.28	0.85
2,500	37.80	22.36	0.89	2.70
3,000	65.61	38.81	1.85	5.50
3,500	98.47	58.25	3.23	9.70
4,000	136.40	80.68	5.12	15.36
4,500	179.36	106.10	7.575	22.73
5,000	227.40	134.51	10.67	32.01
5,500	280.50	165.91	14.5	43.5
6,000	338.60	200.30	19.07	57.21

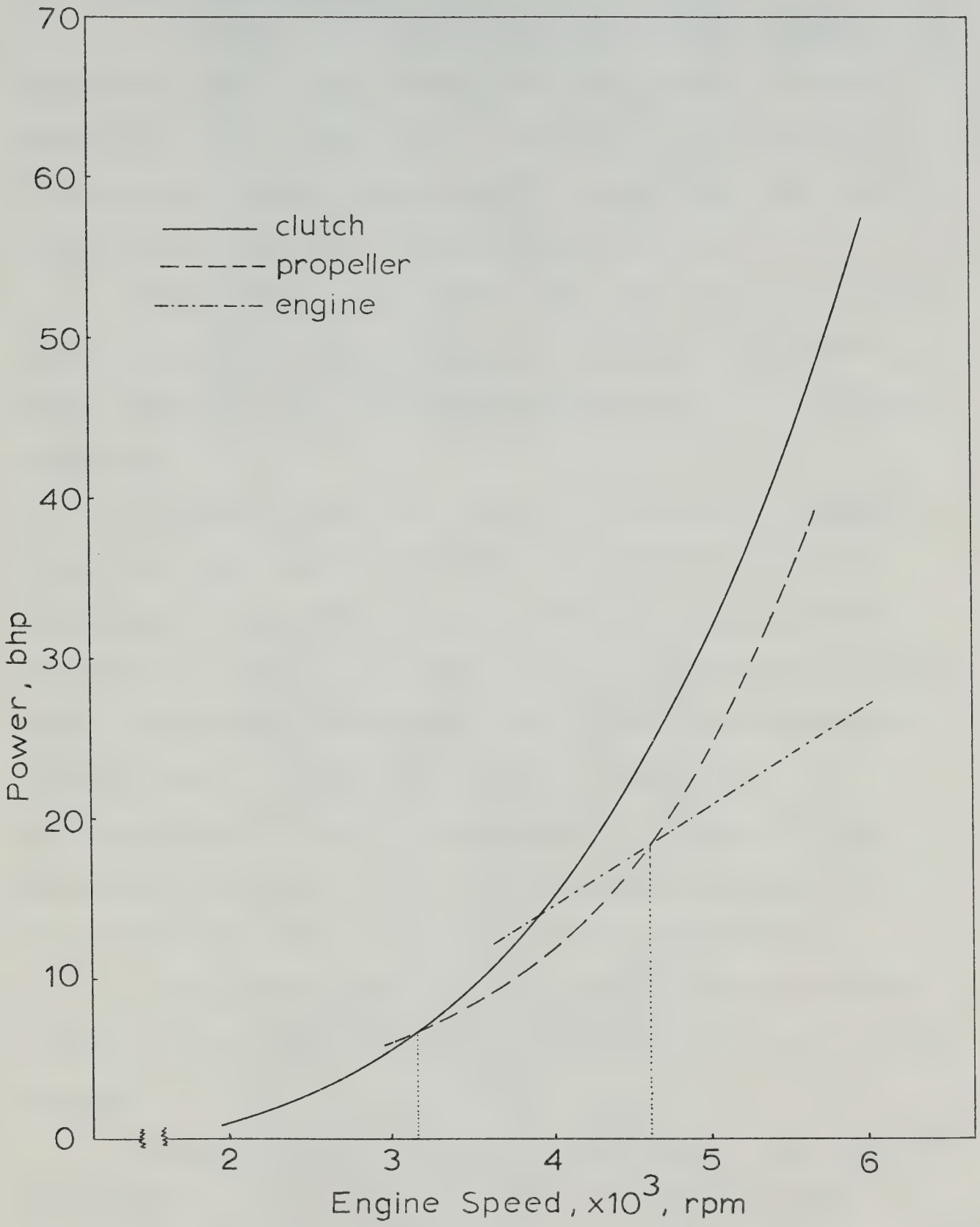

FIGURE 15, POWER TRANSMISSION CAPABILITY OF CENTRIFUGAL CLUTCH

7.4 Power Transmission

The power is transmitted by means of a timing belt drive with a speed reduction ratio of 2:1 at the propeller shaft. The use of timing belt eliminates the initial belt tension that would be needed with Vee belts, thus reduces the radial load on the bearings.

The width of the timing belt was limited by the width of the sprocket, which was limited to two inches by space available for the retraction mechanism in the glider fuselage.

A Morse timing belt of 1/2" pitch and 2" width (complete specifications; 100PL-1000H-200) was chosen. According to the information in Morse Catalogue CSP-74, this belt is capable to transmit 43.64 horsepower at 6,000 rpm. Since the maximum power available from the engine is 27 horsepower, the minimum factor of safety is 1.61. A safety factor of two is recommended for industrial use, but since the engine will not be operated continuously at full power the safety factor of 1.61 is acceptable.

The smaller sprocket was obtained locally and the bigger one was custom built out of aluminum plates to save weight.

Maximum shear stress in the propeller shaft would be 4,600 psi. In a transmission shaft, the torsional deformat on should be limited to 1 degree in 20 diameters [8], while in the present case it is 0.87 degrees in 20 diameters.

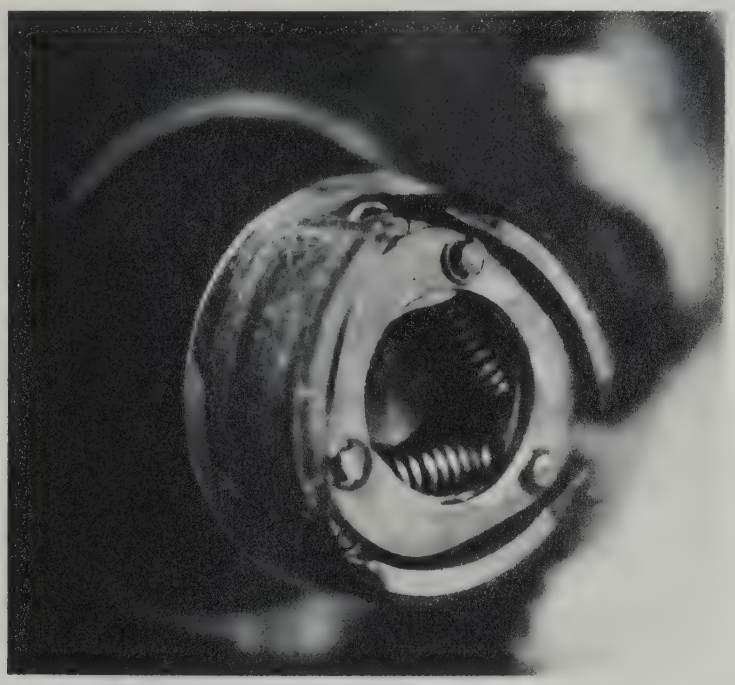

FIGURE 16 , PHOTOGRAPH OF CENTRIFUGAL CLUTCH

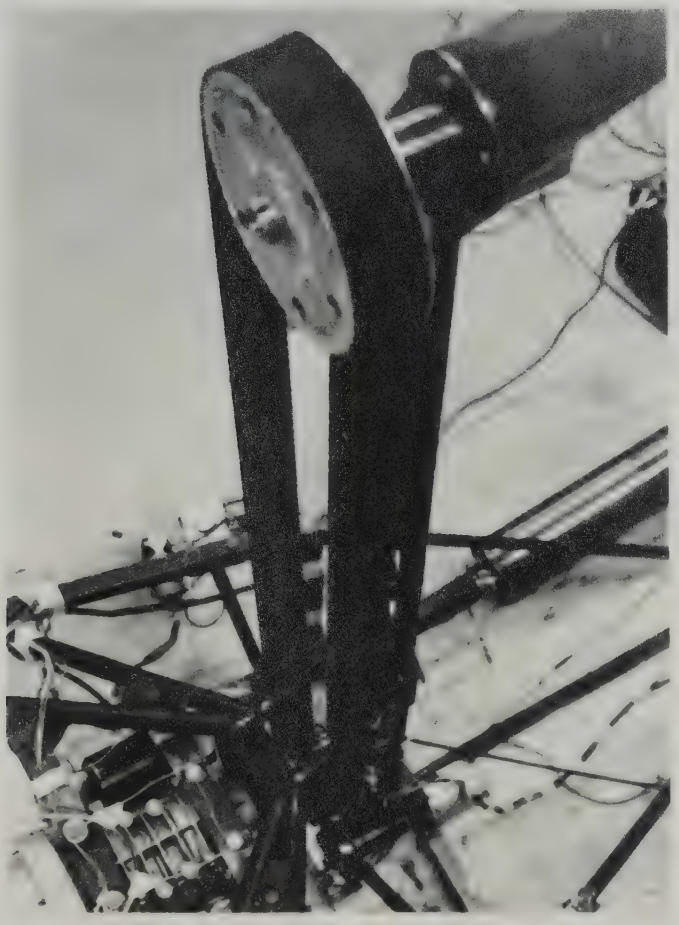

FIGURE 17 , PHOTOGRAPH OF DRIVE SYSTEM

Torque is transferred to the propeller by four, 1/4" diameter steel bolts. The maximum shear stress in each bolt would be 2,000 psi.

7.5 Support Structure and Engine Mount

The support structure (Figure 18) is made from 1 inch O.D. and 0.035 inch wall thickness, 4130 aircraft steel tube. This structure takes up a maximum forward load of about 750 pounds through the upper support, and also it supports the weight and reaction torque of the engine. It transmits the load to the fuselage through a 1 inch square steel tube which goes horizontally around the main body. A theoretical analysis of this structure could not be done because of its complex shape.

The engine is mounted on two heat treated spring steel strips. During the test runs, these strips were found to be not stiff enough. Stiffer mounts would reduce engine vibrations.

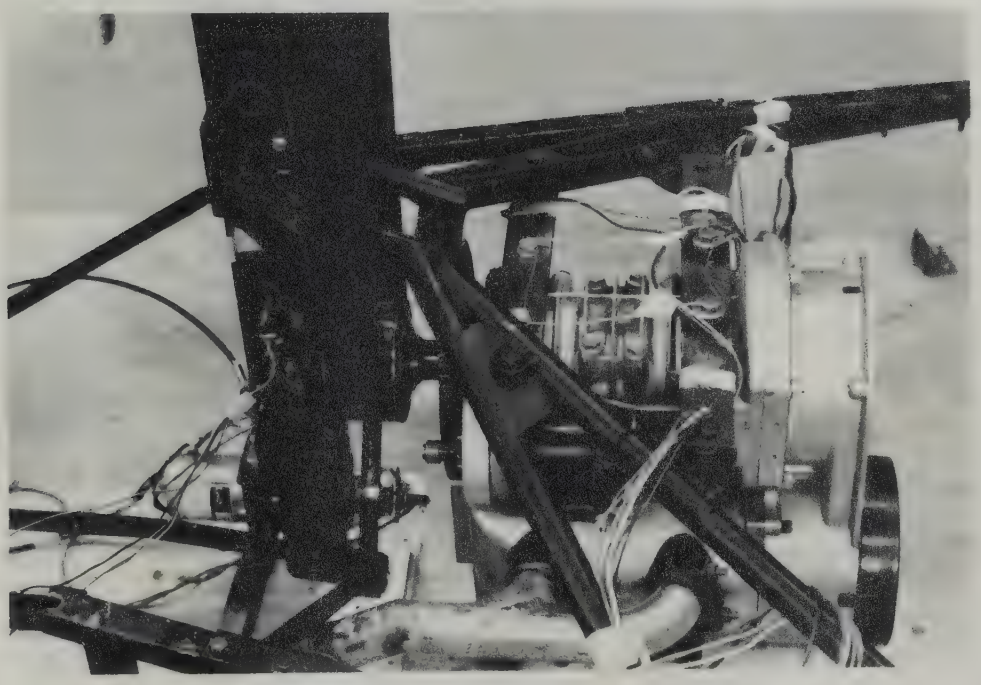

FIGURE 18 , PHOTOGRAPH SHOWING
SUPPORTING STRUCTURE AND
ENGINE MOUNT

CHAPTER VIII

TEST PROGRAM

8.1

The following parameters were measured:

i. Thrust.

ii. RPM of the propeller and the engine.

iii. Air Velocity.

iv. Engine Power.

8.2 Instrumentation

8.2.1 Thrust Measurement

Thrust causes a bending stress on the pylon, and strain gauges placed on front and rear faces near the point of maximum bending moment were used to measure thrust.

Details of the strain gauge circuit and estimates of sensitivity are shown in Appendix IV. Using a four arm active bridge, 120 ohms strain gauges and 5.0 volts dc input, the range of output was calculated to be from 70 μV to 12.25 μV for the load range of 1 pound to 225 pounds. The voltage over this range can conveniently be detected with the help of Hewlet Packard 3490A Multimeter with digital read out.

The output of the strain gauge circuit was cali-

brated by applying known loads horizontally through the center of the propeller shaft. The output was consistent and free from hysteresis. Figure 19 shows the calibration curve for thrust.

8.2.2 RPM Measurement

A General Radio 1538-A strobotac was used to measure the rpm of the propeller as well as the engine. Besides being convenient to handle, it was used to observe any slip of the centrifugal clutch. The strobotac scale could be read with an accuracy of ± 5 rpm.

8.2.3 Air Velocity Measurement

The low speed wind tunnel was used to measure the variation of thrust with forward velocity.

The velocity profile across the wind tunnel test section was measured, and found to have variations of ± 5 percent with velocity peaks near the walls of up to 13 percent higher than the mean flow speed. Although the quality of airflow in this large test section is not as good as it might be for wind tunnel tests, it should be adequately uniform to give valid test results for these propeller tests.

The maximum average airspeed over the propeller area was 32 knots, measured with the help of a pitot static tube and an inclined manometer.

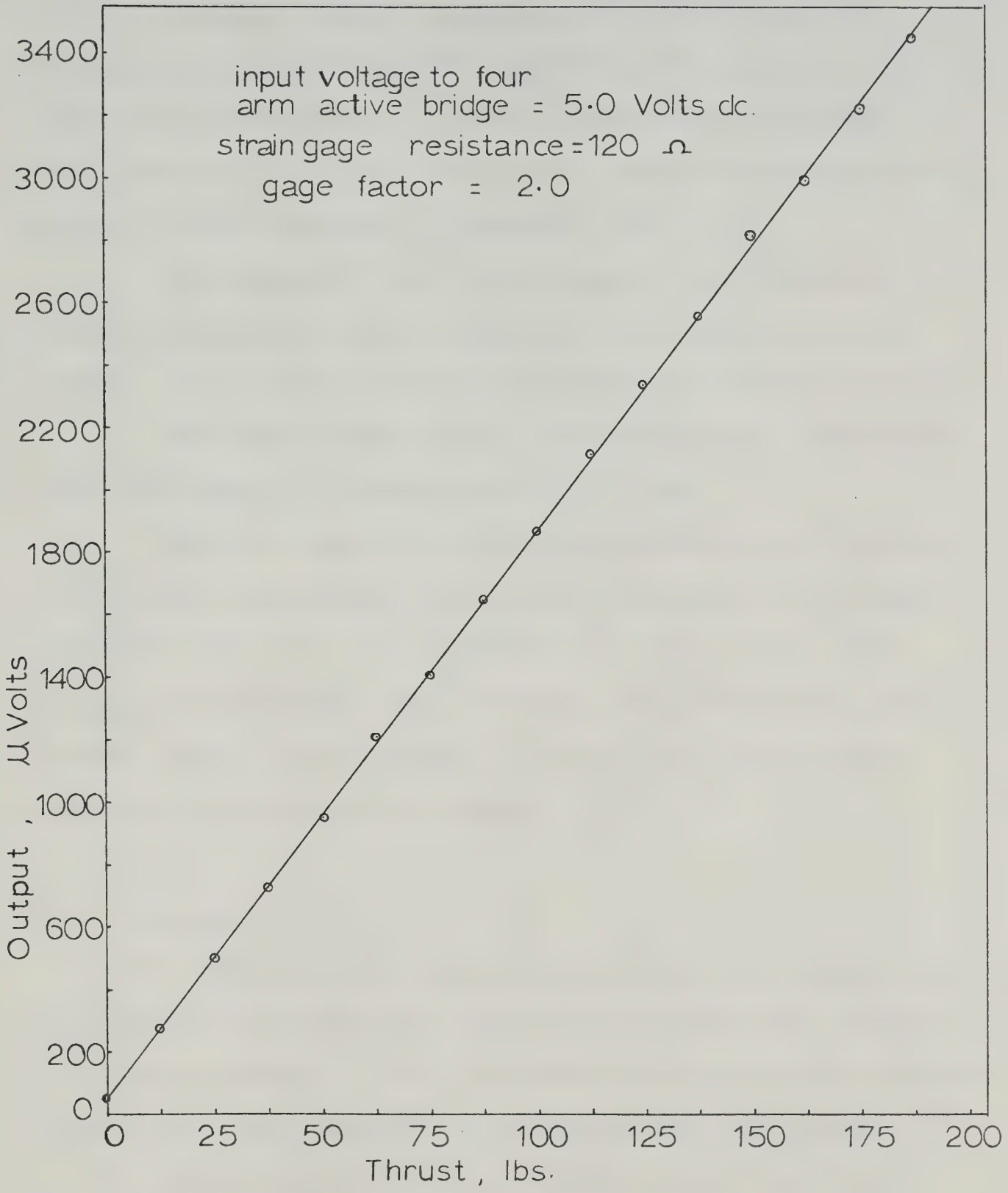

FIGURE 19, CALIBRATION CURVE FOR THRUST

8.2.4 Power Measurement

Reaction torque was measured with the help of strain gauges placed on the engine mounting strips. The range of the strain variation in these strips is from 50 μ inch/inch to 230 μ inch/inch. Details of the strain gauge circuit are shown in Appendix IV.

The output of the strain gauge circuit was calibrated by applying known torque at the crankshaft of the engine. Figure 20 shows the calibration curve for torque.

The input power can be calculated with the help of reaction torque of the engine and its rpm.

Bearing losses are only about 0.25 percent of the total power consumption [9]. Exact information on losses in timing belts is not available. An estimate of about 96 percent efficiency [8] was made. Thus the total transmission losses were assumed to account for approximately 4.25 percent of the total power.

8.3 Test Runs

The complete unit was mounted on one inch square tube framework which simulates the framework structure in the fuselage of Gemini. This test bed was anchored down to the floor of the low speed test section of the wind tunnel.

The exhaust system consisted of a 22 inch long flex pipe, a silencer, a fan blower and about 25 feet of 3 inch diameter stove pipe. The fan blower compensated for the back pressure caused by the silencer and the long stove

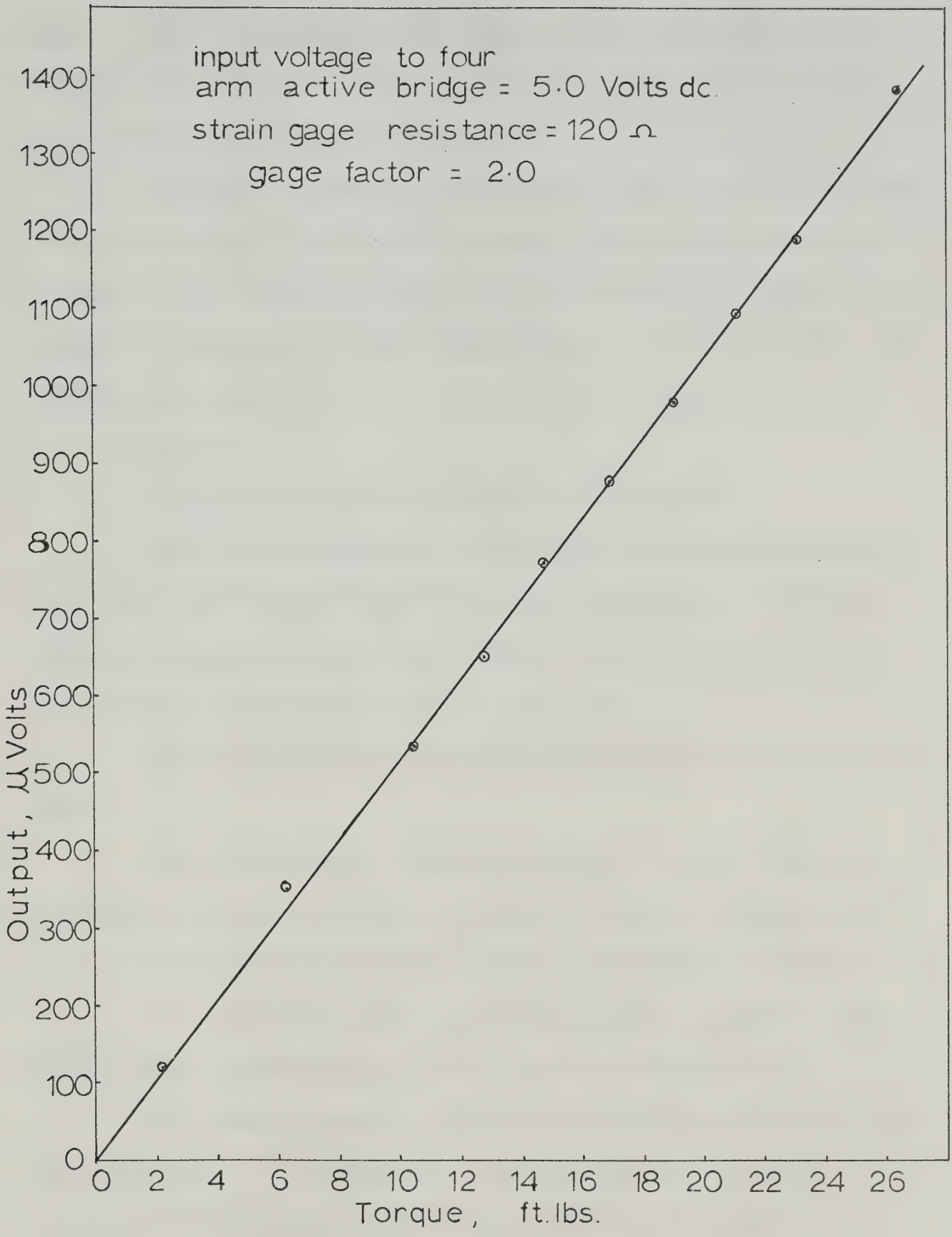

FIGURE 20, CALIBRATION CURVE FOR TORQUE

pipe. This arrangement was found to work satisfactorily in that noise levels were low and all the exhaust gases were piped out of the wind tunnel.

Throttle control of the engine was located outside the wind tunnel. Any engine speed could be achieved within ±5 rpm of the desired speed over the operating range of the engine. The engine idled smoothly at 1,400 rpm. This is the maximum speed at which the shoes of the clutch stay fully closed in.

Test results are tabulated in Table 2.

The retraction mechanism operated satisfactorily. When the pylon comes into an upright position, the lower sprocket covers the clutch without interfering with the shoes at the idling speed of 1,400 rpm.

Some modifications were made following the initial tests.

The diameter of the hinge pins in the clutch was increased from 0.2 inches to 0.3125 inches, because of failure of 0.2 inch diameter pins due to fatigue loading.

The two forks which provide upper support to the pylon, were reinforced to take up transverse load.

The lower support for the end of the pylon was not rigid enough. It deflected considerably when thrust exceeded 100 pounds, and this caused misalignment of the clutch and the drum. After reinforcement, this support became fairly rigid so that no appreciable deflection was observed.

The two square tubes which provide test bed for the system and simulates the Gemini fuselage, tended to deflect laterally outward as a result of load on the lower support. A tension member was welded at the end of the frame to check the deflection.

Maximum speed of the propeller at zero forward velocity was found to be 2,450 rpm, and at 32 knots it was 2,520 rpm.

8.4 Corrections in Thrust and Power Measurement

Tension in the belt causes a bending moment on the pylon which adds to the bending moment due to forward thrust. Drag of the pylon causes a bending moment opposite to that of thrust. Therefore, the indicated thrust reading requires correction for the belt tension and for the pylon drag.

The belt tension was obtained from the reaction torque on the engine. The distance of the strain gauges from the thrust line is 2.70 feet. The center line of the belt is 2.5 inches from the neutral plane of the pylon. The coefficient of drag for the pylon was taken to be 1.2, and an expression for the bending moment of the pylon drag, about the center line of the strain gauge was found to be $1.944 \times 10^{-3} \times V^2$, where V is the airspeed in feet/second.

Corrected thrust was obtained from the following equation formed by balancing the bending moments of the belt tension, drag and indicated thrust, about the center

line of the strain gauges:

$$\text{Thrust}_{(\text{corrected})} \times 2.7 = \text{Thrust}_{(\text{indicated})} \times 2.7$$

$$- \frac{\tau}{r} \times \frac{2.5}{12} + 1.944 \times 10^{-3} \times V^2$$

where τ is the reaction torque of the engine, in ft. lb., and r is the pitch radius of the smaller sprocket, in feet.

The losses in bearings and power transmission were estimated to be 4.25 percent. Therefore the actual power required by the propeller was obtained by subtracting the losses from the total measured horsepower, calculated with the help of reaction torque of the engine and its rpm.

Table 2 lists the experimental results, corrected thrust and corrected horsepower.

TABLE 2

TEST RESULTS

Propeller Speed (rpm)	Average Air Velocity (knots)	Indicated Thrust T(lbs)	Indicated Torque τ(ft. lb)	Belt Tension *τ/r (lbs)	Corrected Thrust (lbs)	Corrected Power (h.p.)
1,600	0	72.5	9.6	60.31	67.8	5.6
	12.7	64.5	9.6	60.31	60.18	5.6
	20.0	54.7	7.0	44.00	52.12	4.1
1,800	0	86.5	10.85	68.17	81.2	7.12
	12.7	84.7	10.85	68.17	79.8	7.12
	15.3	80.0	10.8	67.85	75.24	7.1
	18.5	78.0	9.4	59.05	74.14	6.2
	20.0	76.5	9.2	57.8	72.86	6.03
	32.0	52.43	8.4	52.8	50.46	5.51
2,100	0	126	17.6	110.6	117.47	13.5
	12.7	120	17.3	108.7	111.9	13.24
	15.3	117	17.3	108.7	109.1	13.24
	18.3	113	17.1	107.43	105.4	13.12
	32.0	81.8	13.1	82.30	77.5	10.05

* r = pitch radius of the smaller sprocket.

TABLE 2 (CONTINUED)

Propeller Speed (rmp)	Average Air Velocity (knots)	Indicated Thrust T(lbs)	Indicated Torque τ(ft. lb)	Belt Tension $^{*}\tau/r$ (lbs)	Corrected Thrust (lbs)	Corrected Power (h.p.)
2,250	0	148	19.7	123.77	138.5	16.2
	12.7	140	19.2	120.63	131.02	15.74
	32.0	105.56	16.45	103.30	99.7	13.50
2,400	0	172	19.5	122.5	162.55	17.10
	32	130	18.0	113.09	123.4	15.75
**2,450	0	193	21.0	131.94	182.8	18.76
2,500	32	146	21.5	135.08	137.7	19.6
***2,520	32	151	21.5	135.08	142.7	19.75

* r = pitch radius of the smaller sprocket.

** Maximum Static Performance.

*** Maximum performance at 32 knots.

CHAPTER IX

DISCUSSION

Test runs were designed to test the reliability of the whole unit and to measure the performance of the propeller and the engine. Initial testing for about seven hours revealed certain weak points which were improved for further tests.

The timing belt showed flutter problems at high air velocity and high rpm. On one instance the belt rode off the bigger sprocket at 2,300 rpm and 32 knots of air velocity. Fairings around the belt may be needed to reduce the belt flutter.

The centrifugal clutch was supposed to transmit all the power requirements of the propeller above 3,100 engine rpm. During the tests, the clutch was found to be slipping at about 4,700 engine rpm, and above that speed the slip occurred randomly, in sudden little jumps. The engine speed was fluctuating up to $\pm$25 rpm.

The possible reason for the slip was the misalignment between the clutch and the drum, due to deflection of the supports. The misalignment would reduce the area of contact at the friction surfaces, thus causing a jump in speed of the engine.

The misalignment also causes fatigue loading on the

hinge pins. The diameter of these pins was increased from 0.2 inches to 0.3125 inches for that reason.

The misalignment can be prevented by making the pylon supports fairly rigid, and also by checking the deflection of one support relative to the other.

A flexible coupling between the engine and the clutch would check vibrations between them.

Experimental data was established up to 2,500 propeller rpm 32 knots of air speed. Figure 21 shows the comparison of measured performance with the theoretical one.

The trend of change in thrust and power with forward velocity is quite similar to that predicted. The measured thrust is in good agreement with the calculated thrust.

The curves of thrust as a function of forward speed shown in Figure 21 have been extrapolated to zero forward speed by means of the approximate relationship given by equation 5.8. The resulting values of static thrust are in good agreement with measured values at propeller speeds up to 2,250 rpm. The extrapolated value at the highest propeller speed of 2,450 rpm was 9 percent lower than the measured static thrust.

Standard deviation for a group of seven points on the thrust curves where forward velocity exceeds induced velocity, is 3.4 pounds. Measured thrust varies within ± 5 percent of the calculated values.

Power required at higher propeller speed is approximately 10 percent less than predicted by theory. Since

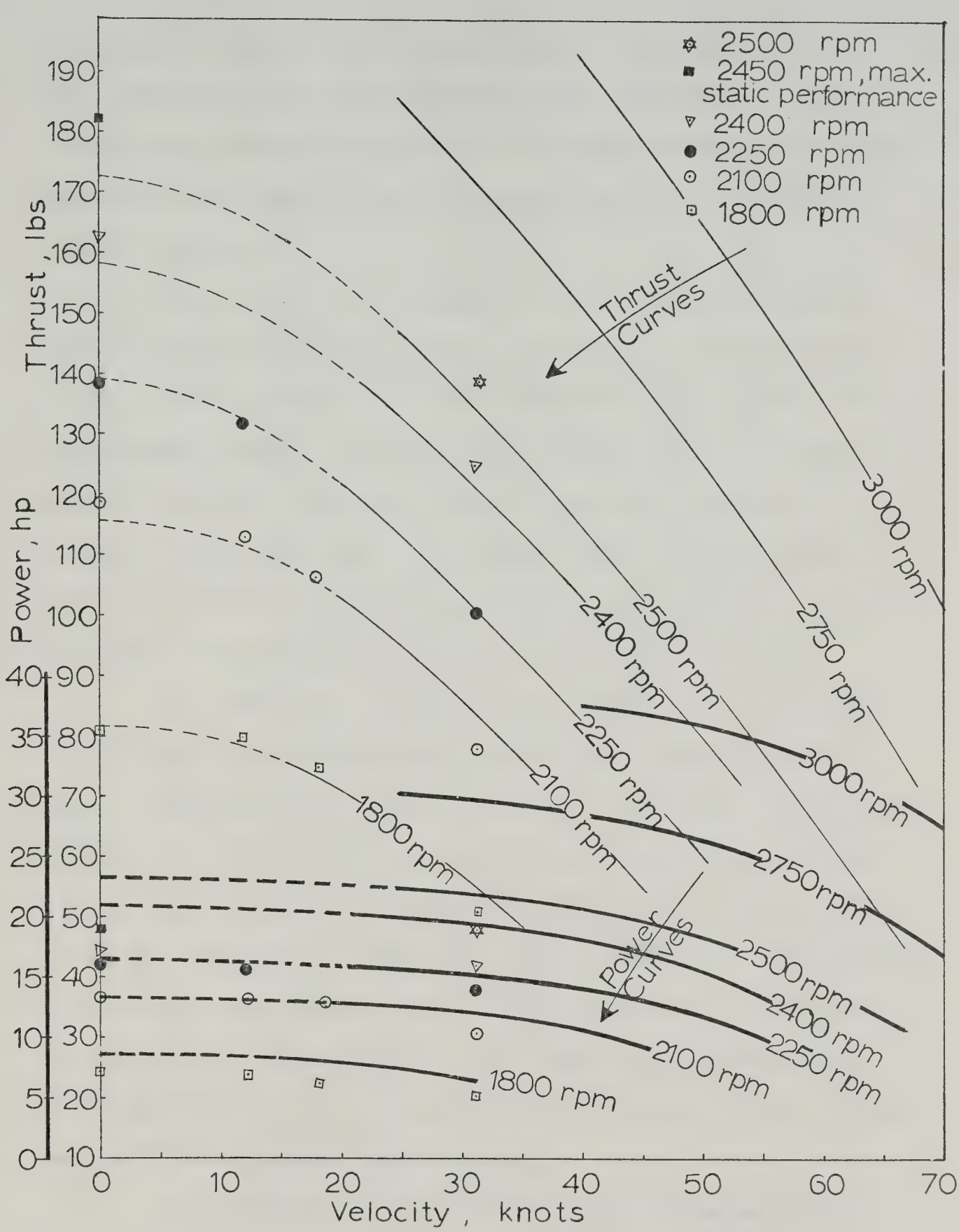

FIGURE 21 , PROPELLER CHARACTERISTICS AND MEASURED PERFORMANCE

the maximum engine power measured was in good agreement with dynamometer measurements at the same speeds, the difference between predicted power requirements and those measured are probably due to approximations in the propeller theory.

The effect of changes in lift to drag ratio is very small as compared to that of changes in lift curve slope. For example, at 2,500 propeller rpm and 30 knots of forward speed, a 300 percent increase in L/D causes 4.6 percent drop in power and about 2 percent increase in thrust. Reducing only lift curve slope by 10 percent, from 0.1 to 0.09 per degree, produces 7.5 percent decrease in power required and 6 percent decrease in thrust.

Any decrease in assumption of the value of lift curve slope does reduce the theoretical power required, but it decreases the thrust as well. If power calculations match well with the experimental results, thrust values differ appreciably. A suitable value of lift curve slope could be selected so that the thrust and power calculations are within acceptable limits of approximately 10 percent. In the present case, L/D of 50:1 and lift curve slope of 0.09 would bring the theoretical performance within 10 percent of the measured performance.

The propeller characteristics provide an approximate means of matching the engine and the propeller for the desired performance. Knowing the type of aerofoil section of the propeller blades, its performance can be calculated with good approximation.

CHAPTER X

CONCLUSIONS

i. Performance characteristics calculated for this system were verified by wind tunnel tests.

ii. Power available was less than anticipated partly because the motor produced less power than the manufacturer claimed it would, and partly because the propeller chosen had a too coarse pitch to allow the motor to reach its best power speed. However, the power obtained would be sufficient for take off and climb at better than minimum required by the O.S.T.I.V. air worthiness requirements.

iii. The pitch of the propeller, specified by the manufacturer, was 30 inches. This pitch was based on blade angle measured from the flat lower surface of the blade. For calculations of propeller characteristics, the zero lift line angle was added to this angle. The true pitch was about 41 inches.

iv. The maximum static thrust to power ratio was found to be 9.7 pounds per horsepower.

v. The retraction mechanism worked satisfactorily.

The test runs showed that the pylon support structure must be fairly rigid to avoid misalignment of the clutch when thrust loads are high.

vi. The time of conversion from unpowered mode to powered mode is seven to ten seconds, provided the engine is already started.

vii. The dry weight of the unit is 115 pounds. A fuel supply of 50 pounds would be sufficient for about two and a half hours of powered flight. The battery weight of about 25 pounds is in addition to that. Therefore, the entire system would weigh about 200 pounds. The stress calculations for wing structure should be reviewed to see if the additional weight can be carried safely.

viii. The length of the cut out in the fuselage for the pylon is only two and a half feet, which is about 55 percent of the propeller diameter. Despite being a small cut out, it will affect the strength of the aft fuselage which should be reinforced.

ix. Installation of this unit would move the center of gravity of the glider about two and a half inches toward the rear.

BIBLIOGRAPHY

1. McMasters, John H., "The Optimization of Kremer Competition Manpowered Aircraft", Proceedings of Second International Symposium on the Technology and Science of Low Speed and Motorless Flights, MIT, September 11-13, 1974.

2. Hoerner, S.F., "Fluid Dynamic Drag", S.F. Hoerner, New Jersey, 1965.

3. Marsden, D.J., "Gemini - A Variable Geometry Sailplane", C.A.S.J., March, 1975, Vol. 21.

4. Houghton, E.L. and Brock, A.E., "Aerodynamics for Engineering Students", Edward Arnold (Publishers) Ltd., 1974, pp. 99, 118-123.

5. Mises R.V., "Theory of Flight", Dover Publication, Inc., New York, 1959, p. 149.

6. Seely, F.P. and Smith, J.O., "Advanced Mechanics of Materials", John Wiley & Sons, Inc., New York, p. 466.

7. Shigley, J.E., "Mechanical Engineering Design", McGraw-Hill, 1972, pp. 585-591.

8. Doughtie, V.L. and Vallance, A., "Design of Machine Members", McGraw-Hill, New York, 1964, p. 181.

9. "Bearing Technical Journal", F.M.C. Corporation, Indianapolis, 1970.

APPENDIX I

CALCULATED GLIDE POLAR DATA OF GEMINI [3]

Velocity ft./sec.	V_{sink} ft./min.	C_D	C_L	Pylon Drag lbs.
(a) Flap Retracted				
121	209	0.0144	0.50	23.8
110	177	0.0160	0.60	19.8
95.5	145	0.0202	0.80	15.0
85.5	130	0.0253	1.00	11.8
(b) Flap Extended				
77.65	142	0.0365	1.20	9.8
72.6	133	0.0427	1.40	8.5
67.5	131	0.0515	1.60	7.5
64	133	0.0623	1.80	6.5
60.8	138	0.0760	2.00	6.0

APPENDIX II

PROPELLER DATA

Diameter - 54 inches

Pitch - 30 inches, measured at 3/4th of radius

Material - Birch Laminated Wood

Propeller Blade is divided into nine elements in order to calçulate propeller characteristics.

Blade Element Radius (inches)	Element Chord (inches)	Blade Angle (degree) Measured from Zero Lift Line
10	4.24	24
12	4.20	23
14	4.175	21.5
16	4.035	21
18	3.81	20
20	3.51	19
22	3.235	18
24	2.94	17
26	2.64	16

APPENDIX III

ENGINE DATA

Model	-	KOHLER 440 - 2AX
Type	-	Two cylinder, in line, alternate firing, air cooled, two cycle
Displacement	-	436 CC
Carburator	-	Diaphragm type
Crankshaft Extension	-	30 mm 1:10 taper and 1/2" 20 UNF internal thread
Ignition	-	Low tension flywheel magneto with external high tension coils
Lighting Coil	-	123 watt, 12 volt A.C.
Direction of Rotation	-	Counter clockwise viewed from PTO end
Fuel	-	Premium grade, mixed with SAE30 2 cycle engine oil, mixture ratio 40:1
Approximate Net Weight	-	72 pounds, including electric starter

Power rating is shown in Figure 6 in Chapter VI.

APPENDIX IV

STRAIN GAUGE CIRCUIT FOR THRUST AND TORQUE MEASUREMENT

Four arm active wheatstone bridge was used for thrust and reaction torque measurement.

Five vdc was applied across the bridge so that maximum current through a strain gauge of 120 Ω resistance, does not exceed the limit of 0.03 amperes.

The potential differences across CD is given by (page 71, Electrical Resistance Strain Gauges by Dobie and Isaac);

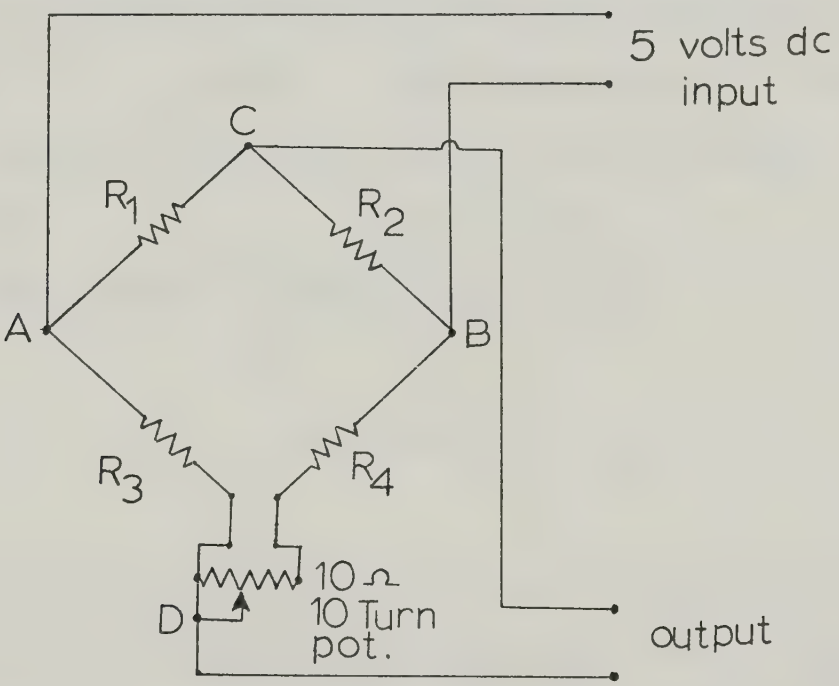

Wheatstone Bridge

$$E_{CD} = E \cdot \frac{R_1R_4 - R_2R_3}{(R_1 + R_2)(R_3 + R_4)} \qquad (1)$$

Small changes in resistance of the strain gauges, because of strain, can be obtained from the definition of gage factor

$$\Delta R = k R \varepsilon \qquad (2)$$

where k is the gauge factor, R is resistance of the strain gauge and ε is strain.

Thrust Measurement

The bending moment on the pylon changes from 32 in.-lb. to 7,200 in.-lb. under a load variation of 1 pound to 225 pounds, thus the bending stress changes between 60 psi and 12,200 psi.

Longitudinal strain is given by:

$$\varepsilon = \frac{\sigma}{E}$$

where σ is stress and E is modulus of elasticity.

The strain varies from 2 μ in./in. to 406 μ in./in., causing ΔR to change between 0.00048 ohms and 0.0976 ohms. Using these values and equation 1, the voltage output range of the bridge is calculated to be 20 μV to 4.06 mV.

The resolution is approximately 19 μV per pound of

thrust.

Torque Measurement

Reaction torque of the engine varies from 100 in.-lb. to 360 in.-lb. Since the engine is mounted on two strips, the reaction torque for each would vary from 50 in.-lb. to 180 in.-lb.

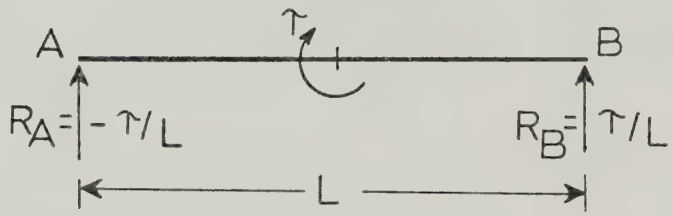

Free body Diagram of Engine Mounts

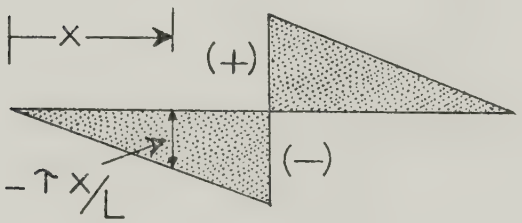

Bending Moment Diagram

For bending moment between 18 in.-lb. and 64 in.-lb., the corresponding bending stress would change approximately from 2,000 psi to 7,000 psi, thus causing the strain to range from 66.7 μ in./in. to 233 μ in./in. The change in resistance of the strain gauges is calculated to be from 0.01599 ohms to 0.05592 ohms, and the output range of the

bridge is found to be from 666 μV to 2.3295 mV.

The resolution of the circuit is approximately 6.5 μV per in.-lb. of torque.